Fall 2017

Study and Implementation of Wideband Bow-Tie Antennas

Md Rakibul Islam

STUDY AND IMPLEMENTATION OF WIDEBAND BOW-TIE ANTENNAS

by

MD RAKIBUL ISLAM

(Under the Direction of Sungkyun Lim)

ABSTRACT

Demand for multifunctional electronic devices is increasing in modern wireless communication systems. As the antenna plays a vital role in wireless communication, the need to design antennas which will provide better performance and more reliable communication is growing. In this thesis, innovative designs for antennas with wideband characteristic have been proposed to meet the demands of current multi-functional wireless communication systems. First, this thesis explores the design of a wideband pattern reconfigurable antenna with steady realized gain over the operating bandwidth. Another novel design of this thesis work is a highly directive wideband Yagi antenna. Finally, a two-planar structured CPLPDA antenna is designed to overcome the currently existing three-planar structured CPLPDA antenna's complex design and fabrication process.

INDEX WORDS: Circularly polarized, Log-periodic antenna, Yagi antenna, Genetic algorithm

STUDY AND IMPLEMENTATION OF WIDEBAND BOW-TIE ANTENNAS

by

MD RAKIBUL ISLAM

B.S., Rajshahi University of Engineering & Technology, Bangladesh, 2013

M.S., Georgia Southern University, 2017

A Thesis Submitted to the Graduate Faculty of Georgia Southern University in Partial

Fulfillment of the Requirements for the Degree

MASTER OF SCIENCE

STATESBORO, GEORGIA

STUDY AND IMPLEMENTATION OF WIDEBAND BOW-TIE ANTENNAS

by

MD RAKIBUL ISLAM

Major Professor: Sungkyun Lim

Committee: Mohammad Ahad

Rami Haddad

Electronic Version Approved:

December 2017

DEDICATION

To my family, friends, and loved ones who have given support, encouragement, and guidance throughout many years of education. For without you, I would not have this wonderful opportunity for personal growth and advancement.

ACKNOWLEDGEMENT

ABBREVIATION

CPLPDA   Circularly Polarized Log-Periodic Dipole Array

GA   Genetic Algorithm

TEM   Transverse Electromagnetic Field

FPCB   Flexible Printed Circuit Board

TABLE OF CONTENTS

LIST OF FIGURES

CHAPTER 1

INTRODUCTION

1.1 Wideband Antennas in Modern Wireless Communication

The modern wireless communication system is an essential part of today's world, and antennas are playing one of the most vital roles in the improvement of the modern communication system's performance. Antenna design has gone through a huge evolution since the antenna was first successfully built by Heinrich Hertz in 1886. Before the late twentieth century, most of the electronic devices used to have a single function compared to modern day when most of the devices are multifunctional. As modern devices use GSM band (850MHZ, 1900 MHz), Wi-Fi (2.4-2.48 GHz, 5.15-5.35 GHz and 5.725-5.825 GHz), WiMAX (2.3-2.4 GHz, 2.495-2.695 GHz, 3.3-3.8 GHz and 5.25-5.85 GH) etc., several small band antennas are needed to embed in the same device for different purposes (Anagnostou, 2013). A router is shown in Figure 1-1 that is equipped with five different antennas, which cover the bandwidth of 2.4 GHz - 5 GHz.

Figure 1-1. TP-LINK N600 600MBPS (TP-LINK)

Although this multi-antenna router serves the purpose of covering the frequency bands required, it is not suitable for portable and compact-size application. Therefore, broadband antennas have become popular due to their size-reduced design while covering many simultaneous wireless applications with a higher data rate and higher reliability of connection. With an increase in the need for more frequency bands for different applications and the growth in demand for better performance and portability of the antenna, research on antenna design is playing an essential role for future development of new high performance wireless communication systems.

1.1.1 Wideband Antenna Background

Typically, the range of frequencies over which the antenna can properly radiate or receive energy is called the bandwidth of an antenna. More specifically, bandwidth (sometimes, is referred to impedance bandwidth) refers to the range of frequencies over which a given S_{11} (reflection coefficient) or VSWR (voltage standing ratio) can be maintained. It can be defined in two different terms: absolute bandwidth and fractional bandwidth. Absolute bandwidth of an antenna is the band difference between the upper and lower frequency of the operating band of the antenna with defined return loss level. Fractional bandwidth is the ratio of frequency difference to center frequency of the operating bandwidth of the antenna (Stutzman, 2013). If the upper and lower frequencies of the operating band of an antenna are f_U and f_L, and f_C is the centre frequency between f_U and f_L, then the absolute bandwidth and the fractional bandwidth can be shown as follows:

$$\text{Absolute Bandwidth,} \; B_a = f_U - f_L \qquad\qquad 1.1$$

$$\text{Fractional Bandwidth,} \; B_f = (f_U - f_L)/f_c \qquad\qquad 1.2$$

Though both bandwidth terms are being used for the same antenna specification, they are used for representing the antenna performance differently. Absolute bandwidth refers to a range of

frequencies where antenna will meet some predefined power transfer specification between the antenna and the transmission line (Stutzman, 2013). The fractional bandwidth of an antenna is a measure of how wideband the antenna is. The fractional bandwidth varies between zero and two, and gives an idea about how wideband the antenna is regardless of the frequency.

Conventionally, the resonant antennas have a lower bandwidth because they mainly have standing waves. Special antenna design techniques to improve the bandwidth, do not emphasize on abrupt changes in the physical dimensions of the antenna. Instead, those techniques emphasizes on using materials which have smooth boundaries that tend to make the input impedance change smoother when changing the frequency (Stutzman, 2013). Specially designed antenna structures prevent wave reflections by using matched loads, and therefore the broadband antennas are also called traveling wave antennas. Typically, antennas with a fractional bandwidth of 20% or more are called wideband antennas. When the fractional bandwidth is 50 % or more then it is referred to as an ultra-wideband antenna (UWB).

When antennas were first introduced by the German physicist Heinrich Rudolph Hertz in 1886, it was a conventional half-wavelength dipole antenna with a narrow bandwidth. With its simple structure and good radiation impedance over the operating bandwidth, dipole antenna is a very popular choice in many wireless communications systems. With the progress of modern communication system's demand for compact-sized devices with more applications being prominent and hence, the demand for compact wideband antennas are also increasing simultaneously.

The very first UWB antenna was a biconical antenna (Figure 1-2) which was introduced by Olive Lodge in 1897 (Schantz, 2004). The biconical antenna shows a broad bandwidth because it uses

the principle of traveling wave structure. Theoretical analysis of this antenna shows that because of the infinite structure of the antenna, it resembles a transmission line. The characteristic impedance at the point of connection for an infinite antenna is a function of only the cone angle and is not dependent on the frequency (Stutzman, 2013). Practical antennas have finite length and a definite resonant frequency.
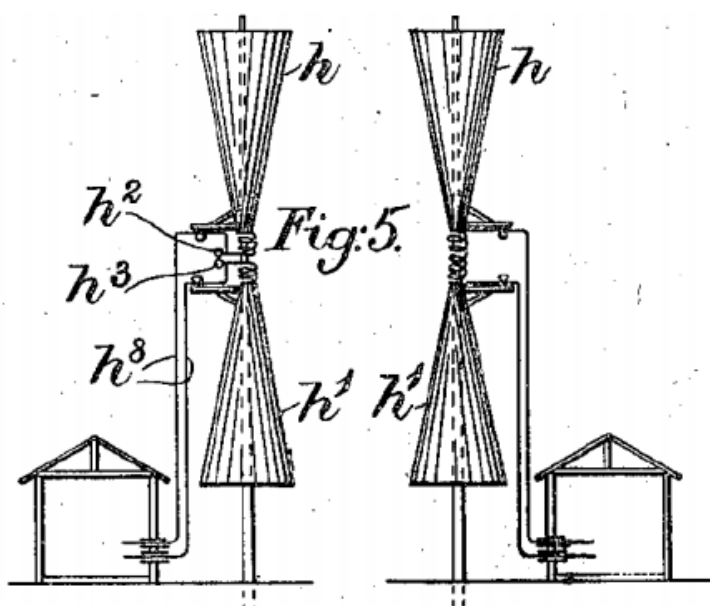
Figure 1-2. Lodge's biconical antenna (Schantz, 2004)

1.1.2   Types of Wideband Antenna

With the advancement of the antenna research, lots of wideband antenna designs have emerged in modern day wireless communication systems. Considering the constraints of space, cost, design and fabrication, and application, various wideband antennas have been designed. Several types of wideband antennas have been listed below in Figure 1-2.
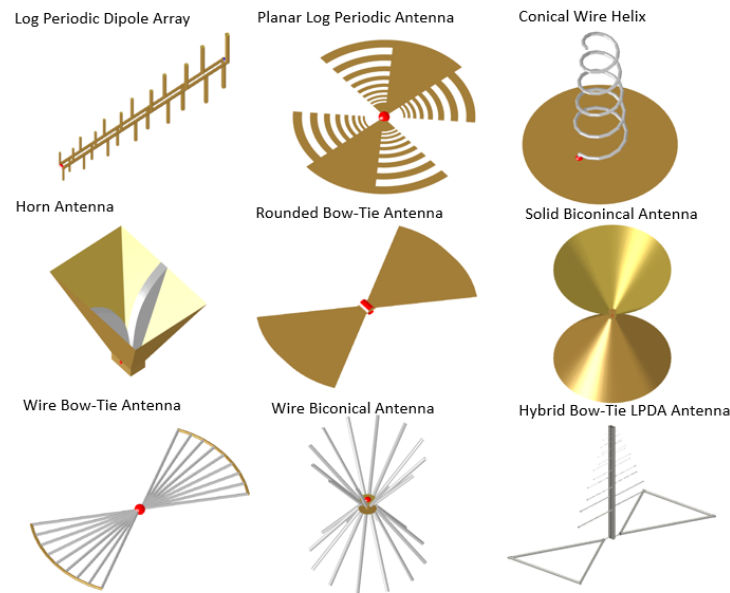
Figure 1-3. Wideband Antennas (Antenna Magus)

Conventional wideband antennas are often spacious, bulky and have a complex design. Chu explored fundamental limits on antenna size, bandwidth, and efficiency (Chu, 1948). According to Chu, antenna will have the widest bandwidth when that they utilize the most space within the circumscribing sphere (Chu, 1948).

Considering all those constraints the planar bow-tie antenna is the best choice for the wideband applications, which is the focus of this thesis.

1.2 Bow-tie Antenna

1.2.1 Bow-tie Antenna Background

As the demand for wideband antennas is increasing, antenna researchers started working to increase the bandwidth of antennas. At first, the concept was to increase the radius of the dipole antenna to increase the bandwidth (Stutzman, 2013), but this bandwidth improvement was not

enough to meet the wideband antenna requirement. This concept can be extended to get further improvement of the bandwidth if the conductors are designed in such a way that they are flared to form a biconical structure. Thus, the fixed wire diameter can be replaced with a smoothly varying diameter with a fixed angle of the conical surface, which helps in achieving wider bandwidth (Stutzman, 2013).
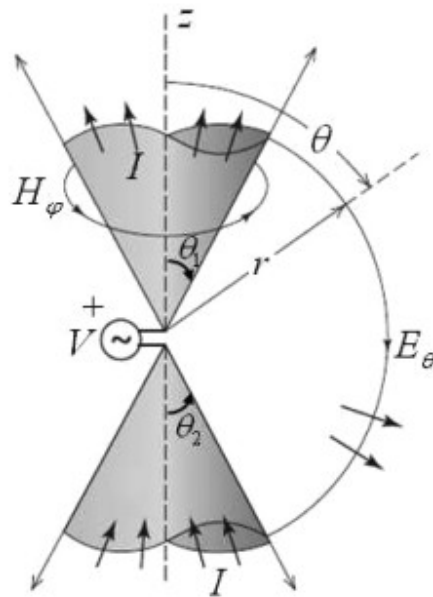
Figure 1-4. Infinite biconical antenna (Stutzman, 2013)

An infinite biconical antenna is a good example of the concept discussed in the previous section. In this design, two infinite conical conducting surfaces end-to-end replaces the two elements of the dipole antenna and a finite gap is kept at the feed point between the two elements (Stutzman, 2013). This antenna structure behaves like a uniformly tapered transmission line as the structure is infinite. When a time-varying voltage is applied across the feed gap, currents flow radially out from the feed point along the surface of the biconical elements. These currents create an enclosing magnetic field, and assuming Transverse Electromagnetic Field (TEM) transmissions line mode, the electric fields will be orthogonal to those magnetic field. This electric field direction is shown

in Figure 1-4. In the spherical coordinate system of the Helmholtz equations, the TEM wave is expressed by the sum of positive and negative exponentials of r (radial distance) which are the conventional expressions for the EM waves traveling inward and outward, respectively, in the radial direction. As the biconical surface is infinite, there is no discontinuity in the radial direction which indicates there will be no reflected wave, and thus broadband characteristics is achieved.
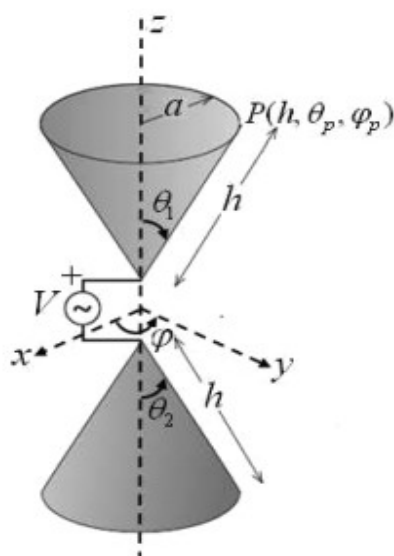
Figure 1.5. Finite biconical antenna (Stutzman, 2013)

Later, a practically implementable biconical antenna was designed by ending the two cones of the infinite bicones which form the finite biconical antenna. Unlike in the infinite biconical antenna where only the traveling wave is present, in finite biconical antennas there are reflected waves present because of the discontinuity at the end of the antenna. Higher order modes of electromagnetic waves (EM) are created by the introduced discontinuity at the end of the finite bicone antenna, which induces a reactive component in the input impedance of the antenna, and thus, the standing wave ratio increases (Stutzman, 2013). By increasing the cone angle θ_h as shown in Figure 1-5, the reactive part of the input impedance can be minimized over a wider bandwidth,

and at the same time the real part of the input impedance becomes more independent of the frequency.
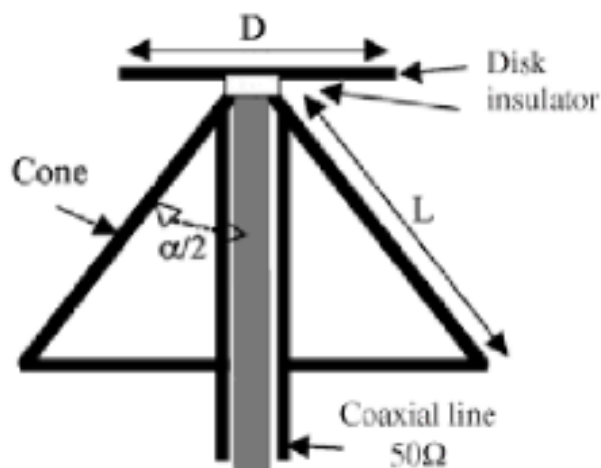
Figure 1-6. Discone antenna (Balanis, 2011)

Discone antenna is an important improvement of the biconical antenna. The discone antenna is a type of biconical antenna in which one of the cones is replaced by a finite disk shape ground plane. In the design of this antenna, the overall diameter of the disc should be equal to a quarter wavelength at the lowest frequency of the bandwidth. The input impedance of a discone antenna depends on frequency and three other geometric variables: the cone's angle, slant length, and the radius of the ground plane disk. At the lower frequencies where the wavelength is longer, the antenna structure especially the ground plane disk is small compared to the wavelength, and therefore, antenna radiation pattern is like a simple dipole antenna (Stutzman, 2013). But as the frequency increases the antenna behaves like an antenna with an infinite ground plane. Because of its wideband coverage, with plain design structure, it is an attractive choice in military, commercial, and radio scanner applications. A discone antenna is shown in Fig 1-6.

The biconical and discone antennas discussed so far in this section are 3D structured and bulky. However, in modern devices, the demand for planar and light weight antennas with reliable

performance is increasing. The bow-tie antenna is a planar version of the finite biconical antenna which can easily be printed on a substrate. As the currents are abruptly terminated at the ends of the bow-tie fins, the antenna has some bandwidth limitation compared to the 3D biconical and discone antennas. Still the bow-tie antenna shows good impedance behavior across a wide band. The VSWR does not degrade significantly as the frequency is increased due to the tapered shape of the bow-tie, and that is why the bandwidth of this antenna depends on the flare angle (shown in Fig 1-7) of the bow-tie.
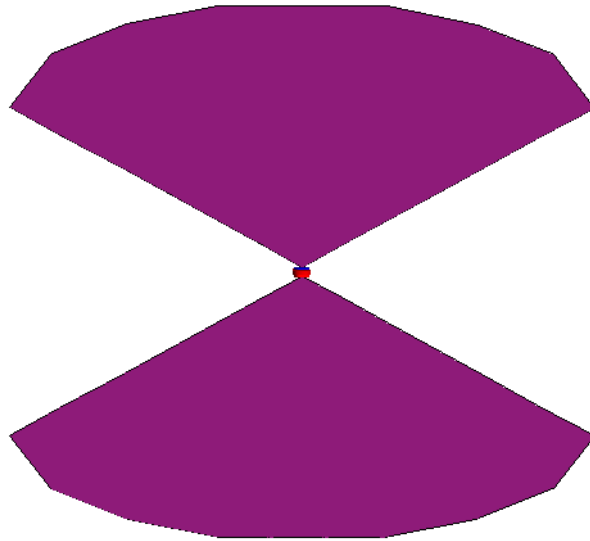
Figure 1-7. Bow-tie antenna

1.2.2   Bandwidth Enhancement Techniques of the Bow-tie Antenna

Introducing tapered metal stub: Compared to wire dipole antennas, bow-tie antennas show wider bandwidth performance. Conventional slot bow-tie antennas show fractional bandwidths of 17-40% (Eldek, 2004). In Eldek's work, by introducing tapering to the metal stubs at the center of the bow-tie slot antenna, a very wide bandwidth enhancement was achieved. In this design using the stub helped to improve the input resistance over the desired wide band, which contributed in

getting better impedance matching. By controlling the stub design parameters, it was possible to shift the main resonance to lower frequency and a new resonance was created in the higher end of the frequency band. Thus, a very wide band was achieved. This antenna is shown in Figure 1-8.
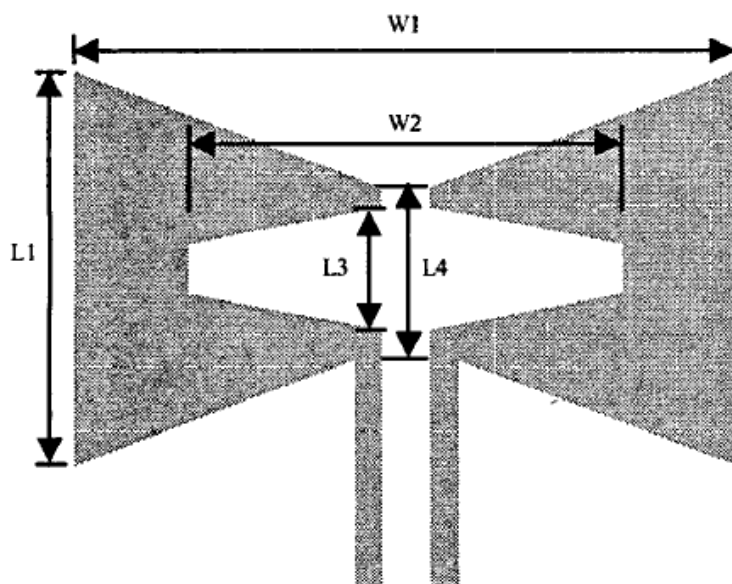
Figure 1-8. Bow-tie with tapered metal stub (Eldek, 2004)
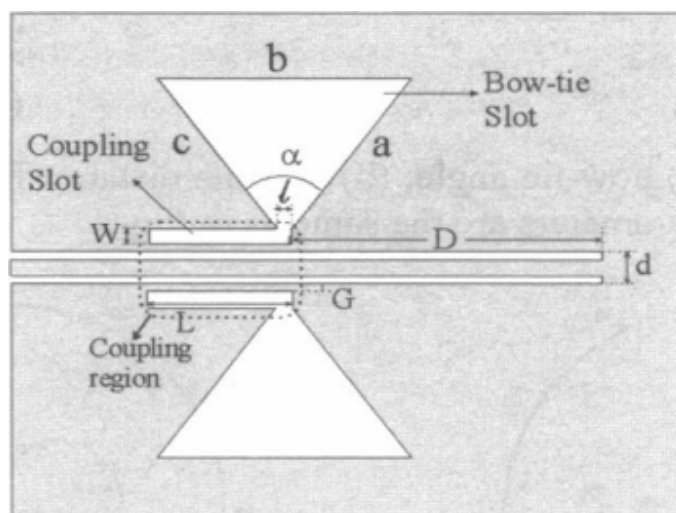
Figure 1-9. CPW feed bow-tie antenna (Shams, 2005)

Coplanar to Waveguide (CPW) feed: The bandwidth enhancement of a conventional bow-tie antenna can be achieved by introducing coplanar waveguide (CPW) feed. This technique helps in

improving impedance matching over a very wideband, and as a result the antenna shows very wideband characteristics (Shams, 2005). The antenna is shown in Figure 1-9.

Introducing multiple flare angle: It is known that the bandwidth of the bow-tie antenna depends on the flare angle. In (Yen, 2016), a bow-tie antenna design (shown in Figure 1-10) is proposed where three bow-tie antennas with three different flare angles are combined. In this design, as three bow-tie antennas have three different flare angles, they operate in three different frequency bands. Since the three different frequency bands are adjacent, when combined they result in a very wide bandwidth.
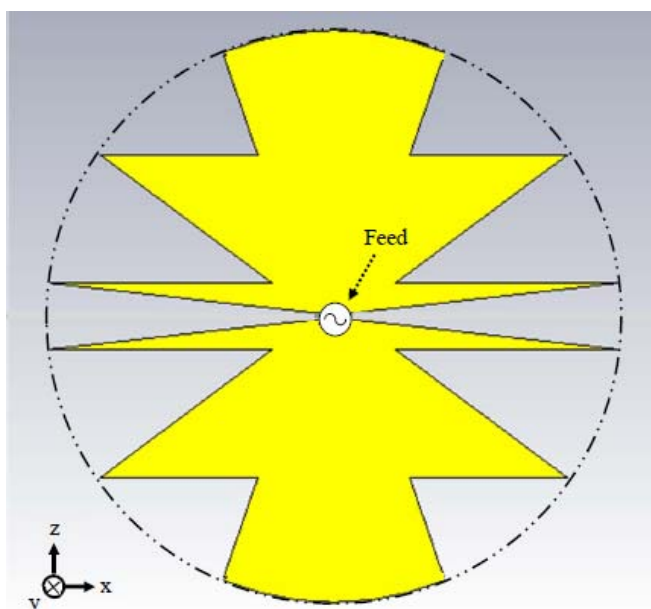
Figure 1-10. Three-element wideband bow-tie antenna (Yen, 2016)

1.3   Pattern Reconfigurable Antenna

A reconfigurable antenna is an antenna which can modify its frequency and radiation properties dynamically in a controlled and reversible manner. Reconfigurable antennas integrate an inner electrical or mechanical mechanism (such as, electrical- RF switches, varactors; mechanical-

mechanical actuators or tunable materials, MEMS) to provide a dynamic response that facilitate the intended redistribution of the RF currents across the antenna surface and provide the capability to modify the targeted antenna property. With the advancement of the modern wireless communication, the need for flexibility in terms of pattern, frequency, and polarization is increasing to achieve versatile and flexible operations in various applications, and reconfigurable antennas offer the best solution for that (Jusoh, 2014).

A pattern reconfigurable antenna for wireless LAN dual-band is proposed (Lee, 2012). In this design, a bow-tie antenna and a wire strip are used as the radiator which are connected by means of chip inductor. As the inductor behaves as a short circuit at low frequency, the radiator of this antenna works as a longer dipole, while only the bow-tie antenna works as the radiator at the upper frequency as the inductor works as an open circuit at the higher frequencies. Though dual-band is achieved, this antenna has the limitation of narrow bandwidth. This antenna is shown in Figure 1-11.
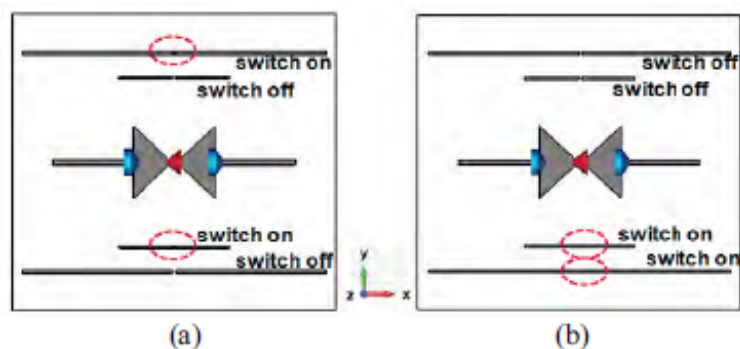
Figure 1-11. Dual-band pattern reconfigurable antenna (Lee, 2012)

Another multidirectional pattern reconfigurable antenna using the bow-tie antennas is proposed (Assimonis, 2015). In this design, a bow-tie antenna is used as the driver and eight other bow-tie antennas are used as parasitic elements surrounding the driver. RF switch is placed between two

arms of the parasitic bow-tie elements, and the operating state of the RF switch is controlled by Double-Pole, Double-Through (DPDT) DC switch. Thus, by controlling the operating state of the parasitic elements, the direction of the radiation pattern is steered to the desired direction. This antenna is shown in Figure 1-12. This antenna has also drawback of limited bandwidth.
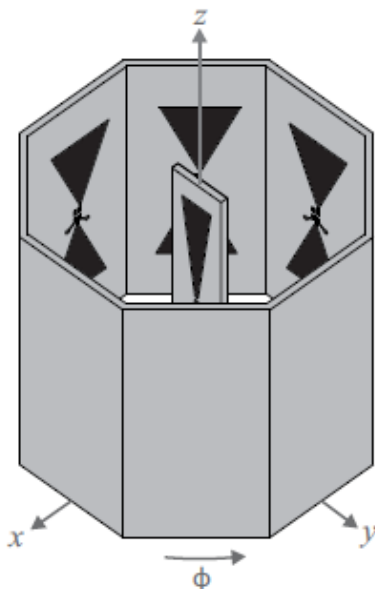
Figure 1-12. Multidirectional pattern reconfigurable antenna (Assimonis, 2015)

In this thesis, a wideband pattern reconfigurable antenna is proposed as the solution to the narrow bandwidth antennas.

1.4 Yagi antenna

A Yagi antenna is a directional antenna consisting of a single driven element connected to feed line, and additional parasitic elements (reflector and director) which are not driven: a so-called reflector and one or more directors. It was first introduced by Shintaro Uda and Hidetsugu Yagi in 1926. The reflector element is slightly longer than the driver, whereas the director element is a little shorter. In this design, as the reflector elements are longer than the driver, it works as an inductive element and the current lags the voltage induced in the reflector. On the other hand, the

director being shorter in length than the driver, it works as a capacitive element and current leads the voltage induced to the director. By selecting correct element lengths and spacing, the radiated radio waves by the driver and those radiated back by the reflector and driver, all arrive at the front side of the antenna in constructive phase, and thus more stronger and directive signal is achieved in the forward direction (director direction). This increases the directivity of the antenna in the director's direction. Though this antenna is a high gain antenna, it has a drawback of narrower bandwidth.

A Yagi antenna design is proposed by D. Arceo *et. al.* to have enhanced bandwidth using bow-tie shaped wire antenna as reflector and director. The principle of this design is to make the driver element and the parasitic elements resonate at three different adjoining frequency bands which will provide wider Yagi antenna bandwidth in combination. The antenna is shown in Figure 1-13.

Figure 1-13. Yagi antenna with enhanced bandwidth (Arceo, 2011)

Using the same concept in Arceo's paper, a much wider Yagi antenna is proposed in this thesis.

1.5   Log Periodic Dipole Array

The Log Periodic Dipole Array (LPDA) antenna was first introduced by Isbell and DuHamel in 1958. This antenna is known as highly directive and very wideband. In the design procedure, the first element's lengths is chosen by selecting a targeted starting frequency of the desired bandwidth and then other elements lengths are calculated using the scale factor (τ) in equation 1.4. Spacing between the elements are calculated using the spacing factor (σ) in equation 1.5. These parameters follow an optimum design graph which is shown in Figure 1-14 (Stutzman, 2013).

The antenna elements length and spacing between the elements are then calculated using the equation below, where *n* is the element number,

$$L_{n+1} = \tau * L_n \qquad\qquad 1.4$$

$$d_n = 2 * \sigma * L_n \qquad\qquad 1.5$$

$$n = 1, 2, 3 \ldots n$$
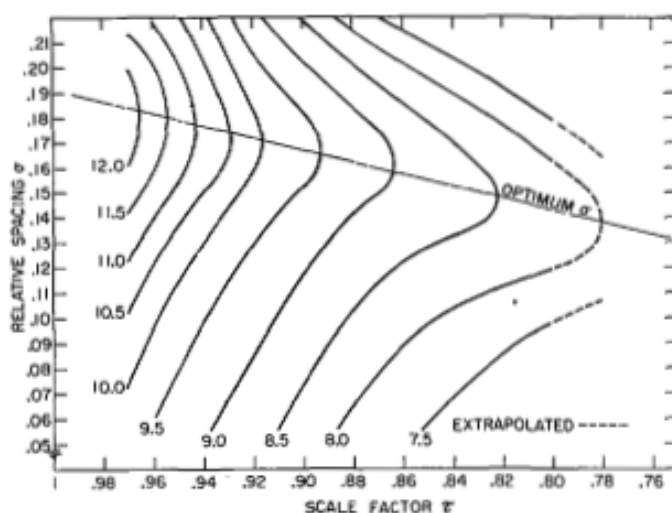
Figure 1-14. Graph of optimum directivity for LPDA antenna versus τ and σ (Stutzman, 2013)
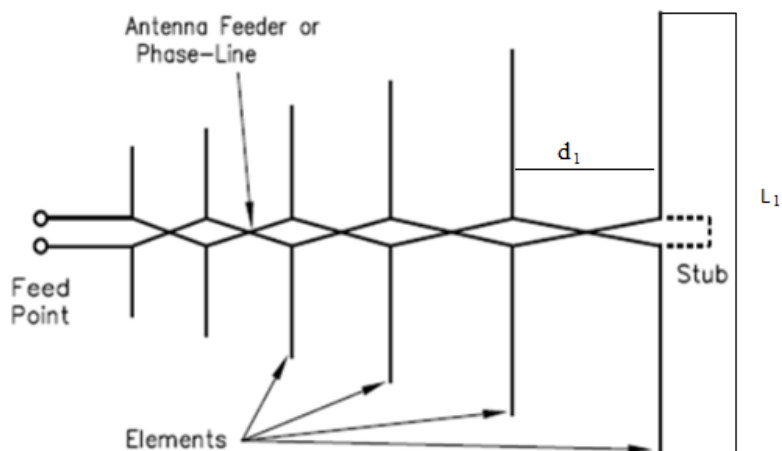
Figure 1-15. Structure of a 6 element LPDA antenna (Stutzman, 2013)

A 6 element LPDA antenna is shown in Figure 1-15. The spacing between the elements and length of the elements, are changing following log periodic manner. Conventionally the fed is in the side of the shortest element.
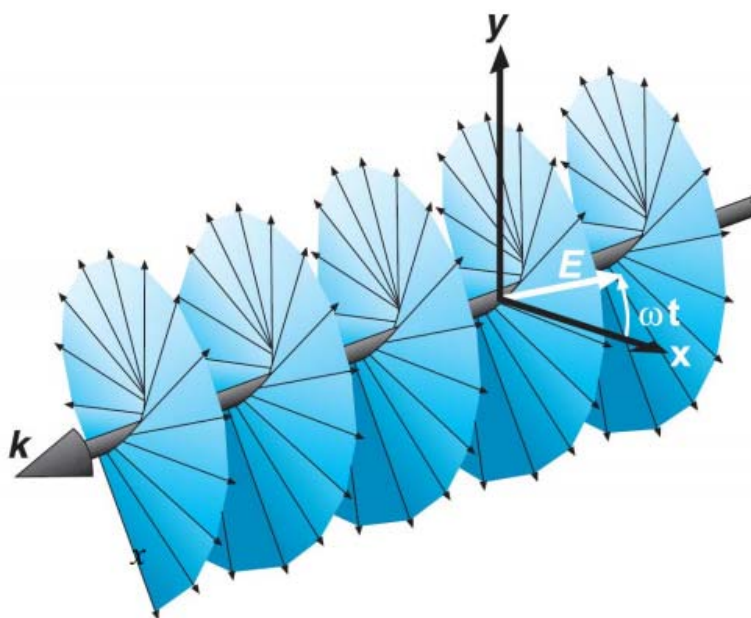
Figure 1-16. Circular Polarization (Hayt, 2011)

1.6   Circular Polarization

The polarization of an antenna is defined in terms of the direction of its electric field vector. If the E-field vector travels along one plane, then it is called linearly polarized. For example, if a monopole antenna is positioned vertically (generally reference to the earth surface), then the E-field will travel along the vertical plane, and if it is placed horizontally, then it creates a horizontal E-field vector propagation. On the other hand, for circular polarization, traveling E-field rotates in a circle while propagating in a specific direction. For generating circular polarization, the antenna should be designed in such a way that it produces two orthogonal E-fields, whose magnitudes are the same but should be 90º out of phase. As a result, the resultant E-field vector travels in a circular pattern to the direction of propagation. When the electric fields are not equal and the ratio is greater than 3 dB then it is called elliptical polarization. Circular polarization is shown in Figure 1-16.

1.7   Antenna Fabrication Instruments and Measurement Setup

1.7.1   Anechoic Chamber
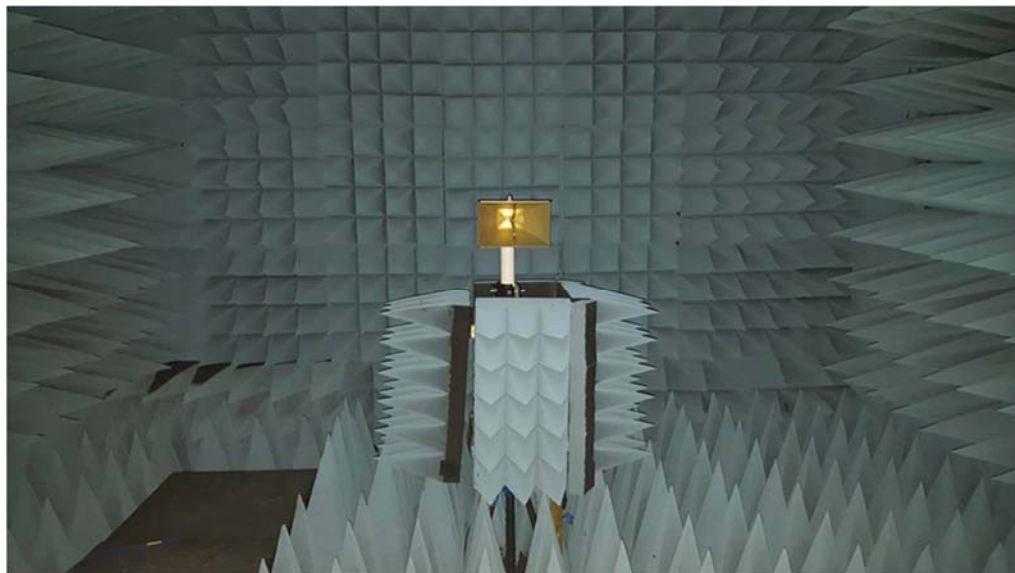
Figure 1-17. Anechoic Chamber

All measurements were done in an anechoic chamber. This chamber's walls are covered with steel plates to suppress any incoming electromagnetic interference, and then cone shaped absorbers to absorb all the electromagnetic waves to prevent any reflection from occurring inside the chamber. This gives the perfect measurement results. The chamber is suitable for measuring antennas with frequency range from 1 GHz to 40 GHz. The anechoic chamber is shown in Figure 1-17.
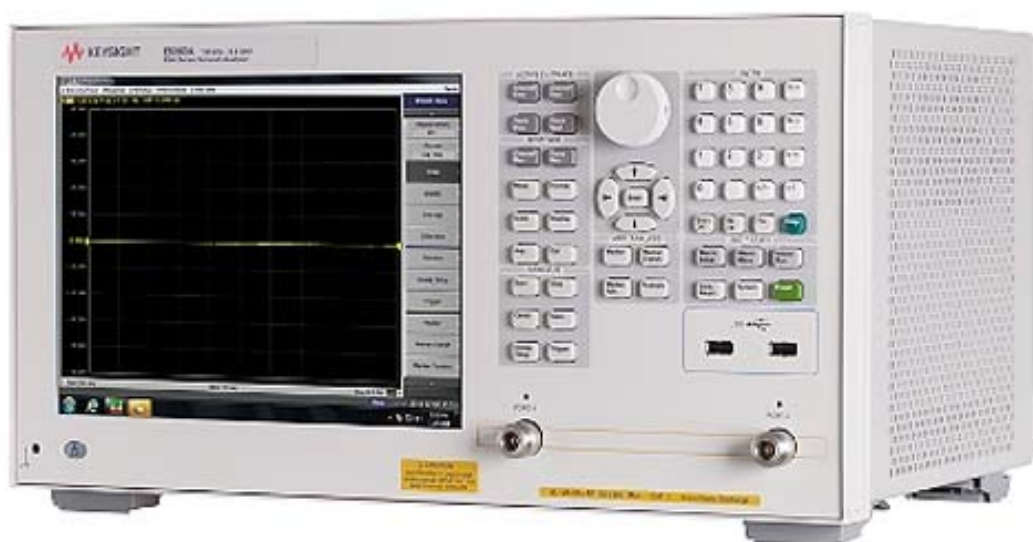
Figure 1-18. Vector Network Analyzer

1.7.2   Network Analyzer

For all the antenna measurements in this thesis, an Agilent ENA E5063A network analyzer is used. It has a measurement range of 100 kHz to 8.5 GHz. It has 2 ports with 50Ω impedance for S-parameters testing, and this port's impedances can be changed to any reference impedance. This network analyzer has both manual and electrical calibration system. Measurements data from this network analyzer are used to plot the S parameter (S_{11}), realized gain, and radiation pattern. Figure 1-18 shows the network analyzer.

1.7.3   KRYTAR 180º Hybrid Broadband Coupler

A balun (balanced to unbalanced) is a type of transformer that can convert an unbalanced signal to a balanced one or vice versa. A balun forces an unbalanced transmission line to properly feed a balanced component. The 180º hybrid broadband balun takes the input signal and divides the power evenly into two separate signals that are 180º out of phase and at the other end of the terminal the signals will then be re-combined together by the internal balancing path and generates balanced output signal. These devices are typically used with broadband antennas. This specific model can perform perfectly from .5 GHz to 7 GHz, and has an insertion loss of 2.8 dB max. The specified model is shown in Figure 1-19.

Figure 1-19. KRYTAR 180ᵒ Hybrid Broadband Coupler

1.7.4   Measurement Setup

Figure 1-20 shows the setup for the antenna measurements. The measurements were taken in the anechoic chamber. The receiver and transmitting antenna were placed 3 m apart from each other.

A TDK horn antenna (HRN-0118) that operates from 1 GHz to 18 GHz is used as a transmitting antenna and this is also called the reference antenna. The testing antenna is in the receiver side. The testing antenna is placed at the top of a rotator to provide a full 360º measurement. The testing and reference antennas are connected to ports 1 and 2 of the network analyzer, respectively.
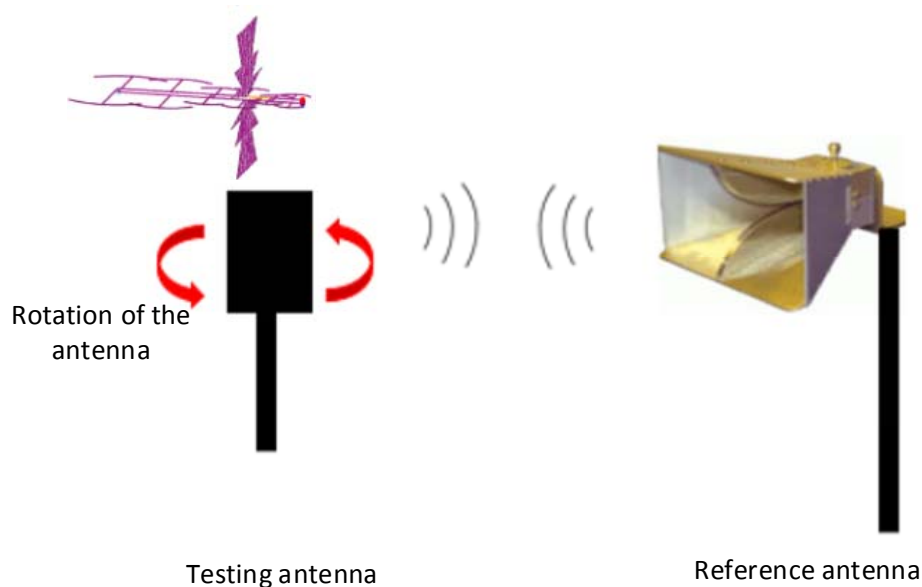
Figure 1-20. Measurement Setup

A computer program controls the rotator rotation and grabs the necessary data for measurement from the network analyzer.

1.7.5   Etching Process

A chemical etching process is used for fabricating the bow-tie antennas. An etching process is preferred because it can provide accurate and superior quality product. Especially for bow-tie antennas that are mostly printed on a flexible substrate material, etching is the only way that could carve the desired antenna design on the flexible printed circuit board (FPCB). A single sided DuPont Pyralux LF 9210R FPCB is used for the fabrication of the antenna. This film contains 2

mils of copper and 1 mil of polyimide film which have a dielectric constant (ξ) of 3.6. The first step of the etching process is to cover the FPCB with a photoresist film and properly laminate the film and FPCB together. Then, the antenna design is printed on a transparent film where the dark area is the etching area and the transparent part is the antenna. After attaching the transparent film on the side of the photoresist film, it is exposed to ultraviolet rays in the E-200 UV screen exposure unit.

(a)   (b)
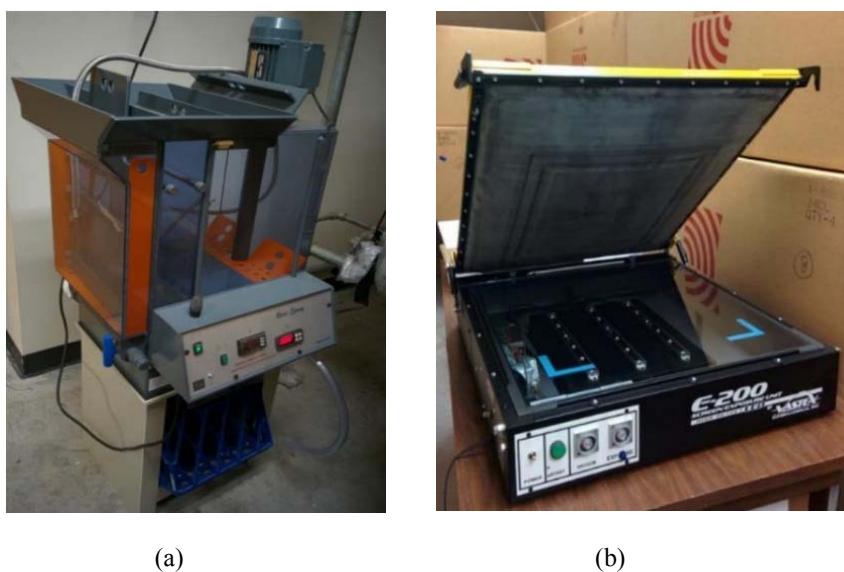
Figure 1-21. Etching Equipment. (a) Rota Spray, (b) UV Exposure Unit

After the exposure, FPCB is placed into developer solution to remove the layer of the unexposed area. Then the FPCB is put in the Rota spray with etching solutions for etching process, and the time for the etching process can be around 30 to 60 minutes based on the acuity and the density of the etching solution. Equipment used in this process are shown in Figure 1-21.

1.8   Thesis objective

The main objective of this thesis is to study wideband bow-tie antennas and design various directive antennas implementing the wideband bow-tie antenna. As the demand for wideband

antennas with pattern reconfigurability is increasing, a novel pattern reconfigurable wideband antenna is designed using bow-tie antenna.

Next, most of the Yagi antennas previously designed have limitation with the bandwidth as this antenna is a directive antenna. In this thesis, a wideband Yagi antenna is designed with high directivity over the whole working bandwidth, while design and fabrication of the antenna was kept simple.

Finally, a 2D structured circularly polarized log periodic dipole array (CPLPDA) antenna is designed using a planar bow-tie antenna and a T-shaped, top loaded LPDA antenna.

1.9   Thesis Organization

Chapter 2 investigates the design of a wideband pattern reconfigurable antenna. A three-element wideband bow-tie antenna is used as the driver element and two triangular bow-tie antennas are used as parasitic reflector. The antenna is designed to provide pattern reconfigurability in two directions. To achieve the pattern reconfigurable characteristics, PIN diode switches are used to electrically turn ON and OFF the connection between the parasitic elements and the ground plane. The proposed design is simulated in the CST microwave studio software, and fabrication and measurement are done for the verification of the simulation results.

Chapter 3 presents the design of a very wideband Yagi antenna. In this proposed design, the conventional Yagi antenna elements are replaced by three-element wideband bow-tie antennas. Different resonances are achieved for driver and parasitic elements, and due to coupling of all three element's individual bandwidths, the combined bandwidth of the Yagi antenna is very wide. The antenna has shown a steady realized gain over the entire bandwidth and little higher realized gain

is achieved in the high frequency area of the achieved bandwidth. This antenna is fabricated, and antenna parameters are measured to verify the simulation results.

Chapter 4 discusses the design of a 2D structured CPLPDA antenna. In this design a T-shaped, top loaded LPDA antenna is used. A three-element wideband bow-tie antenna is placed orthogonally with the T-shaped, top loaded LPDA. The purpose is to achieve wideband circularly polarized antenna with a single feed excitation and matching with a 50Ω characteristic impedance.

Chapter 5 discusses the conclusion of the conducted research work in this thesis and future prospect of the novel antenna designs in this study.

CHAPTER 2

DESIGN OF A WIDEBAND, HIGH GAIN, PATTERN RECONFIGURABLE ANTENNA

2.1 Abstract

A wideband bow-tie pattern reconfigurable antenna is presented in this section. A three-element wideband bow-tie antenna is used as the driver and two triangular shaped parasitic bow-tie antennas with two PIN diode switches are used to direct the radiation pattern to desired direction the achieved impedance bandwidth (BW) is 45.0% (1.45 GHz ~ 2.27 GHz) and the average forward realized gain over the bandwidth is about 7.05 dBi.

2.2 Introduction

Pattern reconfigurable antennas are becoming popular everyday with the advancement of the communication technology, and its application in every aspect of life. As modern cities are growing with skyscrapers which increasing the multipath effect for the signals and with increasing the number of users, the probability of interference is also increasing (Inseop, 2013). Highly directive pattern reconfigurable antennas provide good solutions with less cost and space. A pattern reconfigurable antenna has the potential to improve the system performance by adjusting direction of maximum beam while maintaining the same operating frequencies (Yang, 2007). By maneuvering the beam direction and directing the null position to avoid noise interference, it can increase the coverage area (Inseop, 2013). Maneuvering of an antennas radiation pattern enables the communication system to avoid noise or electronic jamming, to improve system security and save energy by not radiating in unwanted directions (Yang, 2007), (Cai, 2012). The pattern reconfigurable characteristics of an antenna can be attained by different methods, such as

switching feed network, switching the loads and switching current distribution in antenna structure (Inseop, 2013). One of the methods to attain pattern reconfigurable characteristics is by phased array antennas. This type of antenna structure is normally complex, large and costly, which is not compatible in many applications (Cai, 2012). Alternative ways are pursued for designing the antenna like MEMS switches and PIN diodes which are more compatible and useful in antenna design for modern applications.

In this direction many pattern reconfigurable antennas were designed. In (Cai, 2012) and (Inseop, 2013), some multidirectional pattern reconfigurable antennas were designed, but those antennas had narrow bandwidth. A wideband antenna was designed using coplanar waveguide (CPW) feeding in (Li, 2011) which made the design complex and the average gain was 2.92 dBi. Some high gain antennas were designed in (Shi, 2015), (Li, 2015) but the limited bandwidth was an issue. A recent four directional wideband pattern reconfigurable antenna was designed in (Alam, 2015) which showed 34% fractional bandwidth from 1.88-2.64 GHz, but the antenna gain was only around 2.8 dBi.

In this chapter, a wideband, high gain pattern reconfigurable antenna is introduced. The antenna consists of three elements; two reflectors and the driver. This antenna provides wideband, as the driver bow-tie is by itself a wideband, and high gain was achieved as this is a directive antenna structure.

2.3   Antenna Design and Simulation

The proposed antenna uses a three-element wideband bow-tie antenna as the driver. The driver bow-tie antenna is a combination of three parts with three different flare angles. This makes the antenna resonate in three different adjoining frequency bands, which makes the combined

bandwidth of the antenna much wider, where the longest bow-tie antenna covers the lowest band of the whole bandwidth and the shortest bow-tie antenna covers the highest frequency band of the bandwidth. The three-element bow-tie antenna has an omnidirectional radiation pattern. The driver bow-tie antenna is first designed in CST. For the simulation purpose an infinite ground plane is used.

Driver:
ph: 50.67 mm (0.24λ)
dh: 46.63 mm (0.22λ)
d: 20.54 mm (0.098λ)
a: 165.01°
b: 122.61°
c: 96.25 °
r1: 44.13 mm (0.21λ)
r2: 36.0   mm (0.17λ)
r3: 32.92 mm (0.16λ)
Parasitic:
theta: 28.96 °
r: 28.96 mm (0.14λ)
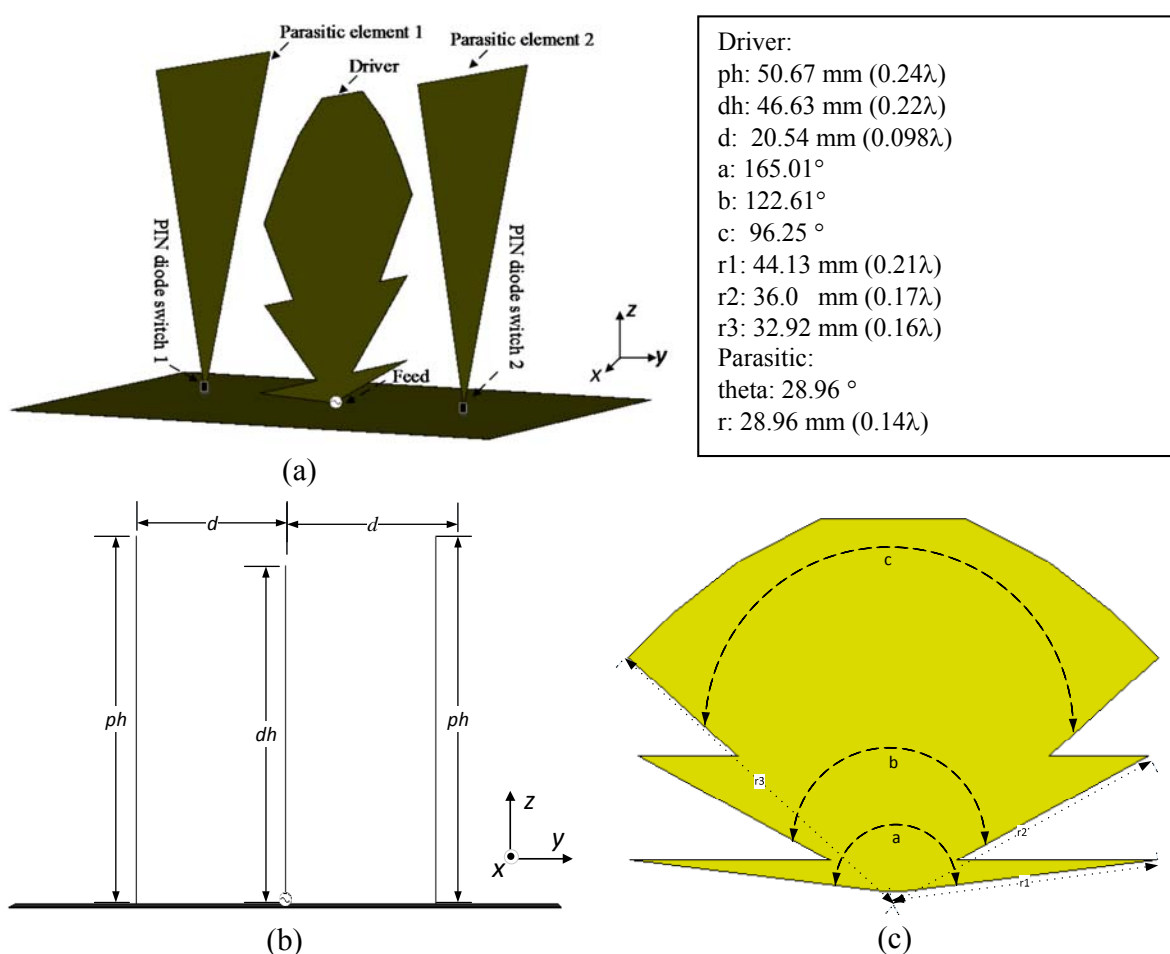
Figure 2-1. Antenna geometry; (a) Slanted view, (b) Side view, (c) Driver antenna parameters

After designing the optimum driver antenna, two triangular bow-tie antennas are used as parasitic reflector to achieve the pattern reconfigurable characteristics. A PIN diode switch is used for changing the pattern reconfigurable states. In this design, for simulation purpose, a PIN diode

switch is realized by introducing a gap between the ground plane and the reflector. This antenna

is reconfigurable in two directions and two PIN diode switches are used for two parasitic reflectors.

The antenna geometry with design parameters is shown in Figure 2-1.
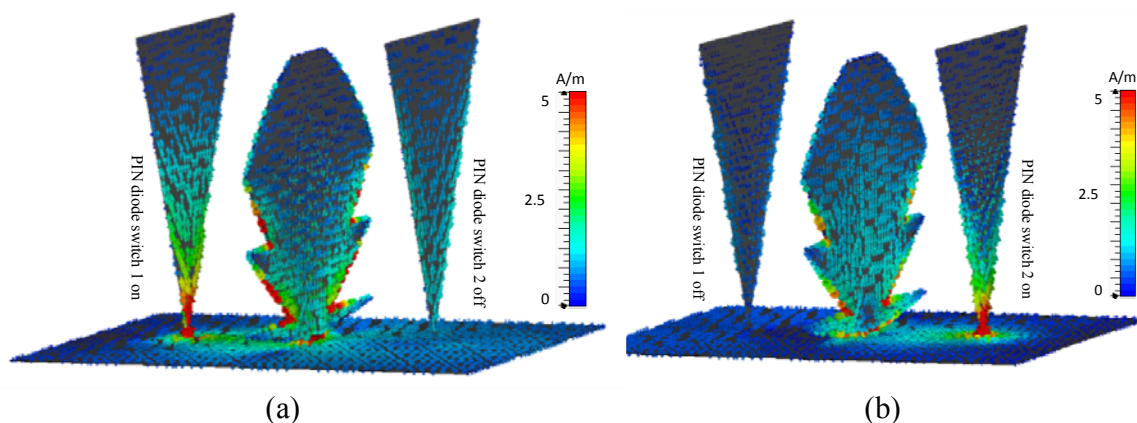
Figure 2-2. Current distribution at 1.5 GHz; (a) PIN diode switch 1 is OFF, (b) PIN diode switch 2 is OFF
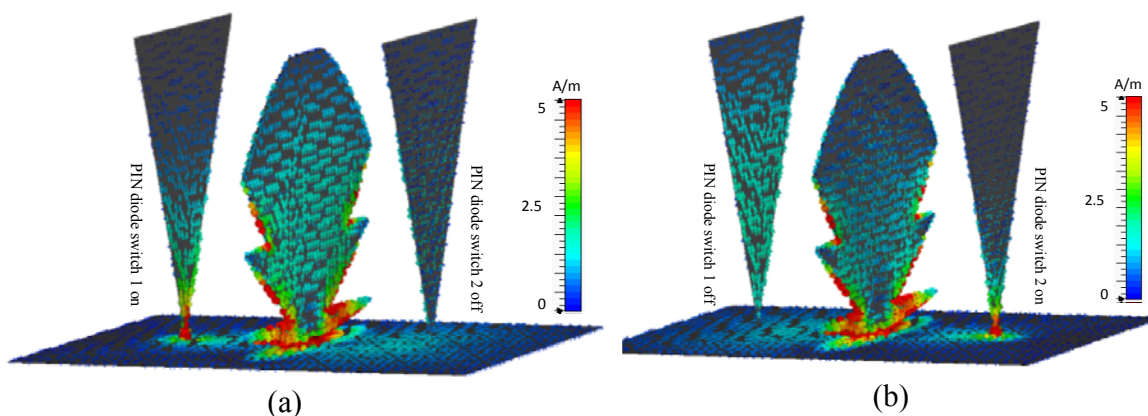
Figure 2-3. Current distribution at 2.2 GHz; (a) PIN diode switch 1 is ON, (b) PIN diode switch 2 is OFF

When the PIN diode switch is ON at phi=0 direction in azimuth plane and PIN diode switch at

phi=180 direction is OFF, then the radiation pattern is directed toward phi=180 direction. In this

condition, the reflector at phi=0 is connected to ground plane through the PIN diode, and it

conducts a strong current. At the same time, another reflector at phi =180 direction works as a

floating element as it does not conduct influential amount of current. The current distribution in

different switching conditions at two different frequencies 1.5 GHz and 2.2 GHz are shown in Figure 2-2 and Figure 2-3, respectively.

From the current distribution, it can be seen that when the parasitic bow-tie antenna is connected to the ground plane, it is getting the strongest current and working as an active reflector. At the same time, the parasitic element in the opposite direction does not have a strong current as it is not connected to the ground, and is working as a floating element with minimum effect on radiation pattern.

The achieved simulated bandwidth is 45 % (1.45 GHz-2.27 GHz), which is shown in the next section with measured results for the ease of direct comparison. Average realized gain is achieved about 7.05 dBi and maximum realized gain is more than 11 dBi in simulation.

2.4   Prototype and Measurement
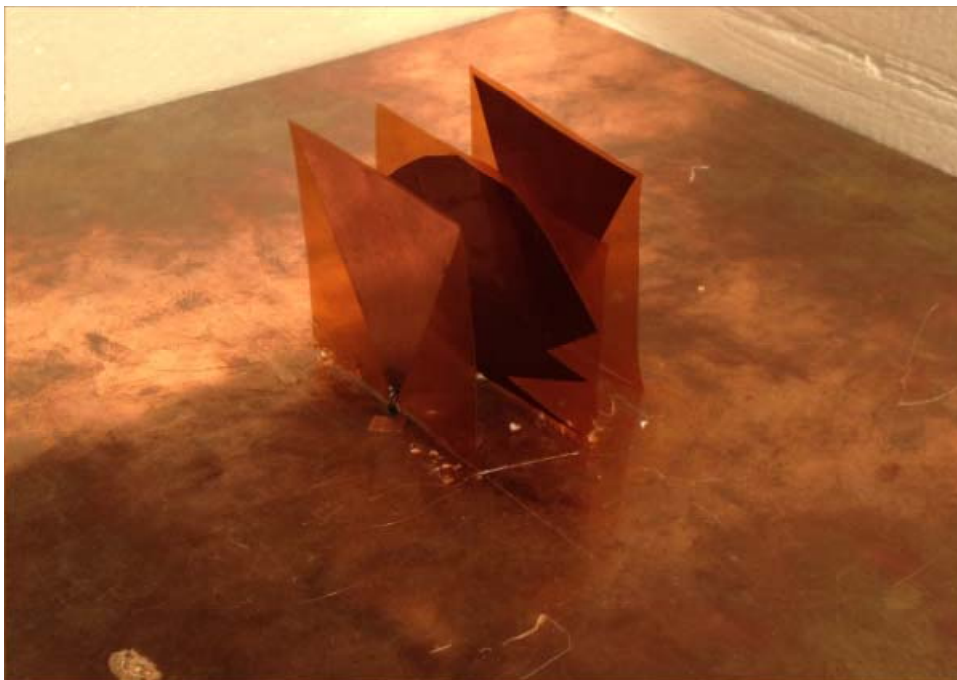
Figure 2-4. Prototype of the antenna

The prototype of the fabricated antenna is shown in Figure 2-4. The ground plane is chosen to be 30 cm × 30 cm (1.44λ × 1.44λ, where λ is calculated at 1.45 GHz, the lowest frequency of the antenna bandwidth). The bow-tie driver and parasitic elements are fabricated on single sided DuPont Pyralux LF 9210R FPCB (copper thickness = 1 mil and ε ≈ 3.6). The parasitic elements are isolated from the ground plane by keeping a gap in between. Parasitic elements are connected to the ground plane through PIN diode switches whose states depend on DC bias applied. The PIN diode switch is driven to ON state by applying DC bias from button cells. At the first step, one PIN diode switch is turned ON leaving the other one OFF. In this condition, S_{11} and radiation pattern is measured. To measure the radiation pattern in opposite direction to the first measurement condition, PIN diode states are reversed, and again S_{11} and radiation pattern are measured.
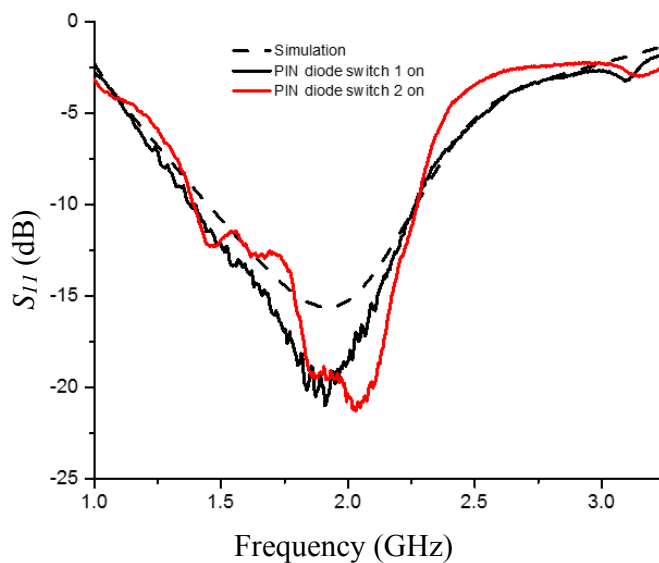
Figure 2-5. S_{11} vs frequency

Measured and simulated S_{11} of the antenna is presented in Figure 2-5. In measurement, the antenna achieves a fractional bandwidth of 46.5% (1.39 GHz-2.27 GHz) compared to that of 45.0% (1.45 GHZ-2.27 GHz) in simulation.

Next, the realized gain of the proposed antenna is investigated. The radiation patterns of the proposed antenna at selected frequencies (1.5 GHz, 1.85 GHz, and 2.2 GHz) are measured. As for the antenna fabrication a finite ground plane is used, in realized gain measurement, next step is to eliminate the finite ground plane effect on the measurement. First, three quarter wavelength monopole antennas resonating at those selected frequencies (1.4 GHz, 1.85 GHz, 2.2 GHz) are fabricated on a finite ground plane that has the same size as the one used for the proposed antenna ($1.44\lambda \times 1.44\lambda$) and radiation pattern at those frequencies are measured, which will be used as references. Then, the realized gain of the proposed antenna can be achieved by subtracting monopole radiation pattern from the measured radiation pattern of the proposed antenna for each corresponding frequency and then adding 4.98 dBi which is maximum simulated realized gain of monopole antenna on an infinite ground plane. By this way the finite ground plane effect can be eliminated (Yu, 2013). The realized gain patterns of the antenna are shown in Figure 2-6 and Figure 2-7 respectively, at three different frequencies across the bandwidth.

2.5   Summary

A wideband pattern reconfigurable antenna with reconfigurability at two directions is proposed. To achieve the reconfigurability of the antenna, PIN diode switches are used and button cells are used for biasing the diodes. A very good agreement is observed between the simulation results and measured results. Achieved simulated bandwidth is 45.0% and measured bandwidth is 46.5%. The antenna achieves an average realized gain of 7.05 dBi towards the desired direction and the maximum realized gain is over 11.0 dBi.

Figure 2-6. Realized gain patterns when PIN diode switch 1 is ON, switch 2 is OFF
(a) at 1.5 GHz, (b) at 1.85 GHz, (c) at 2.2 GHz
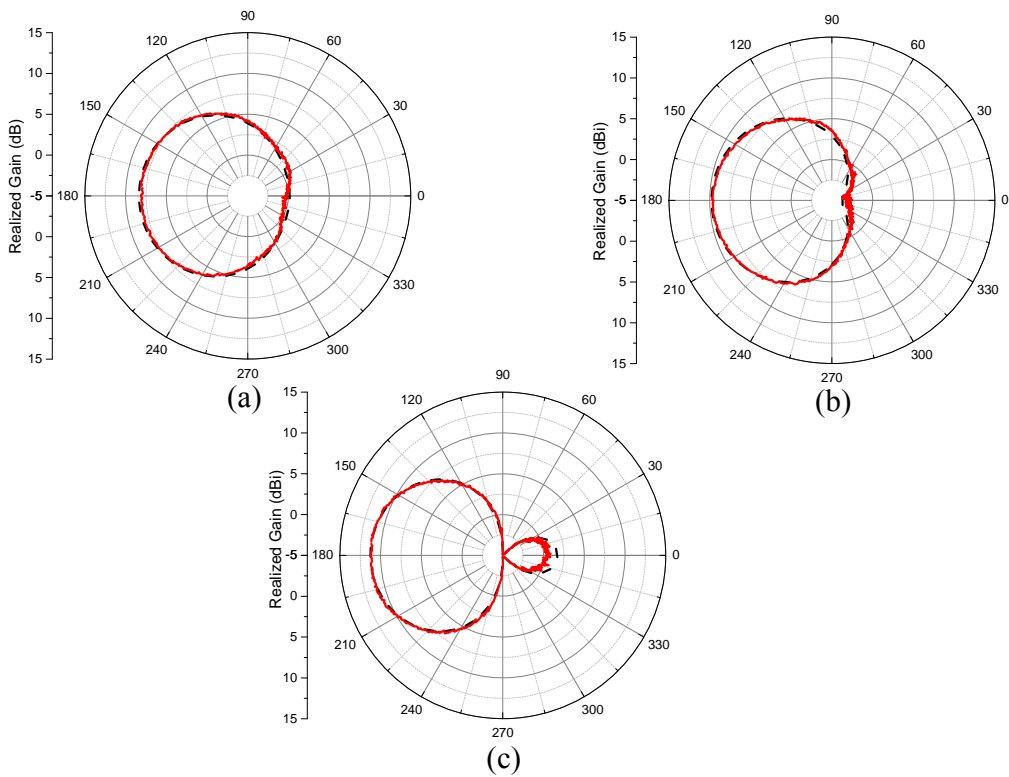
Figure 2-7. Realized gain patterns when PIN diode switch 2 is ON, switch 1 is OFF
(a) at 1.5 GHz, (b) at 1.85 GHz, (c) at 2.2 GHz
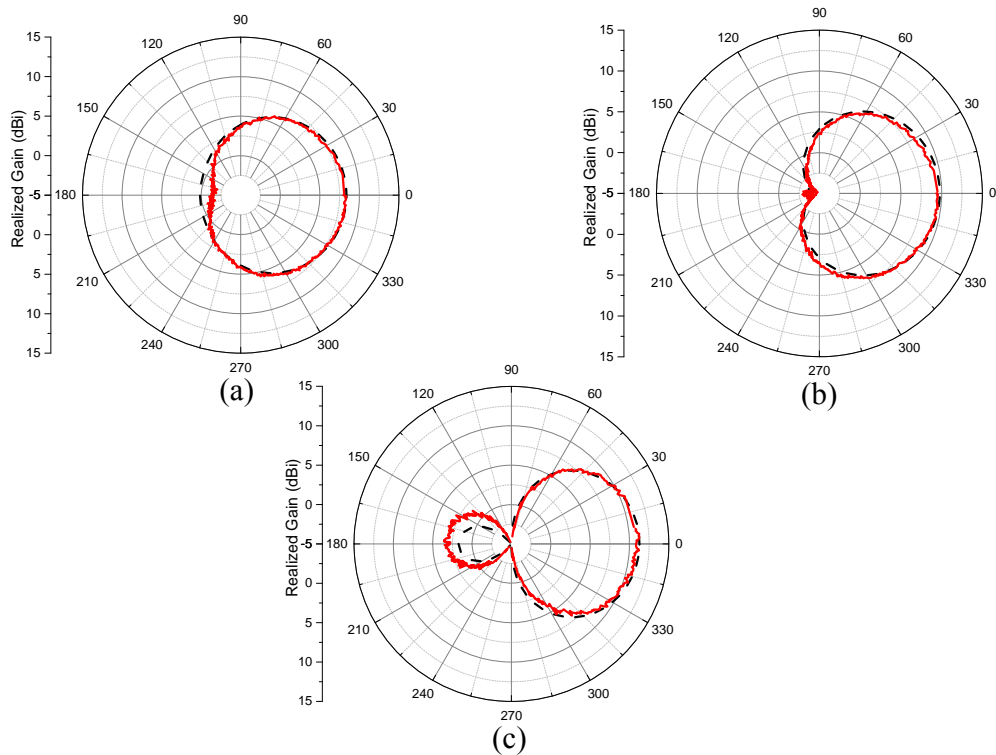
CHAPTER 3

INVESTIGATION OF A WIDEBAND, BOW-TIE YAGI ANTENNA

3.1   Abstract

In this section, a wideband Yagi antenna is introduced. The antenna consists of a driver and two parasitic elements (reflector and director). Three-element wideband bow-tie antennas are employed as the reflector, driver and director. A three-element bow-tie antenna is a combination of three different bow-tie antenna elements with three different flare angles, and thus, provides three different resonances separately in adjoining frequency bands. Hence wide bandwidth is achieved in combination of those three resonant frequency bands (Yen, 2016). In this design, the reflector and director are scaled versions of the three-element bow-tie driver. As the reflector should be electrically larger than the driver, the reflector is the scaled-up version of the driver, while the director is the scaled-down version of the driver. In the proposed design, the wideband reflector and director both improves directivity toward the director's direction while increasing the bandwidth by coupling their own bandwidth with the driver bandwidth. The resulting bandwidth of the proposed antenna is 86% (1.28 GHz– 3.21 GHz). In this design, the distance between the reflector and driver is 40 mm (0.17λ, λ is calculated at 1.29 GHz, the lowest frequency of the bandwidth) and that between driver and director is 15 mm (0.06λ). The realized gain in average over the bandwidth is 9.21 dBi in the director direction and the peak realized gain is 13.29 dBi.

3.2   Introduction

Previously, the Yagi antenna which is a highly directive antenna, was being used for domestic applications, such as receiving signals for televisions. But in current days it is being used widely in various applications in modern wireless communication systems. Because of its high forward

gain capability, with low cost and ease of fabrication, the Yagi antenna is a favored design at VHF and UHF bands. As the Yagi antenna is a highly directive antenna, it conventionally has narrower bandwidth. In (Arceo, 2011), a Yagi antenna is proposed to enhance the bandwidth by using bow-tie shaped parasitic elements. In that design, the overall antenna bandwidth is enhanced by adding the parasitic element's resonance with the driver element's resonance bandwidth and maximum of about 10% bandwidth is achieved. In this direction to further enhance the bandwidth, a Yagi antenna is proposed (Rezaeieh, 2017), using a bow-tie antenna as driver and coupling the parasitic reflector's bandwidth with the driver bandwidth, a 50% fractional bandwidth is achieved.

This chapter proposes a solution to narrow bandwidth Yagi antenna with a novel, directive, and wideband Yagi antenna. The design approach is achieved in two steps. First, investigation is done on antenna shapes that generate wide bandwidth. Then, those antenna structures are used in place of conventional Yagi antenna elements. In this purpose, bow-tie antennas are an excellent choice as a driver antenna for achieving wider bandwidth. In the meantime, to achieve high directivity and gain in the direction of the director, a three-element Yagi structure (reflector, driver, and director) is designed. The proposed Yagi antenna consists of a driven element and parasitic elements (a reflector and a director). Antenna bandwidth is enhanced using a bow-tie shape for the driver and parasitic elements. The antenna is fabricated on a single sided DuPont Pyralux LF 9210R FPCB using Rota Spray etching machine which makes the fabrication process easier and mass production can be done.

3.3   Antenna Design Process

In Figure 3-1, the primary steps of designing the proposed wideband Yagi antenna is shown. At first, a three-element bow-tie monopole [see Figure 3-1(a)] is designed having a bandwidth of 1.30

– 2.31 GHz. In Figure 3-1 (b), a directive antenna design with a reflector and a driver, and in Figure 3-1 (c), another directive antenna using a driver and a director is shown. These two initial antenna designs are to be examined and analyzed to determine the best design parameters of both designs (Design A and Design B) to increase directivity and impedance matching.
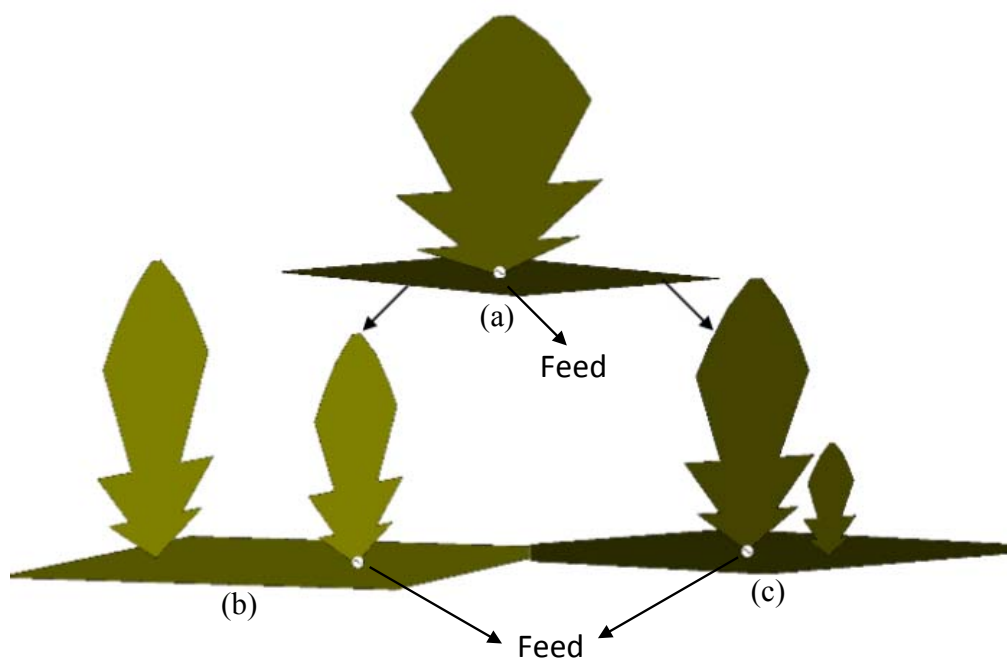
Figure 3-1. Design Steps of Yagi Antenna. (a) Design A: Bow-Tie monopole antenna, (b) Design B: Monopole antenna with bigger element (reflector) added, and (c) Design C: Monopole antenna with smaller element (director) added.

By choosing the parameters wisely, wider bandwidth and high directivity in a desired direction can be achieved in both Design B and Design C. Wide bandwidth is achieved by implementing a bow-tie antenna element as the driver, and the directivity is improved by the parasitic elements. According to the Yagi principle, parasitic element functionality is determined by its electrical size compared to the driver antenna size. Here, the reflector and director are the scaled versions of the driver antenna. The antenna design in Figure 3-1(b), consists of a bow-tie driver and a bow-tie reflector, which is electrically larger than the driver. Therefore, the bow-tie reflector acts as an

inductive element and directs the radiation pattern towards the driver direction. The antenna design shown in Figure 3-1(c) consists of the bow-tie driver and the bow-tie director. Hence, the director acts as capacitive element and directs the radiation pattern towards the director's direction. Both antenna designs in Figure 3-1 (b) and Figure 3-1 (c) are optimized separately by Genetic Algorithm (GA) to achieve maximum directivity and realized gain toward the desired direction (driver direction for Design B and director direction for Design C). Optimization parameters include reflector scaling factor and spacing between the reflector and driver for the design B, and scaling factor of the director and separation distance between the driver and the director for Design C.

The cost function for the optimization is,

$$Cost\ function = \sum_{n=1}^{50}(RG - RG_{ave}) \qquad 3.1$$

Where *RG* is the target realized gain for both antennas and *RG_{ave}* is the average maximum realized gain of fifty equally spaced frequency points within the desired operating band.
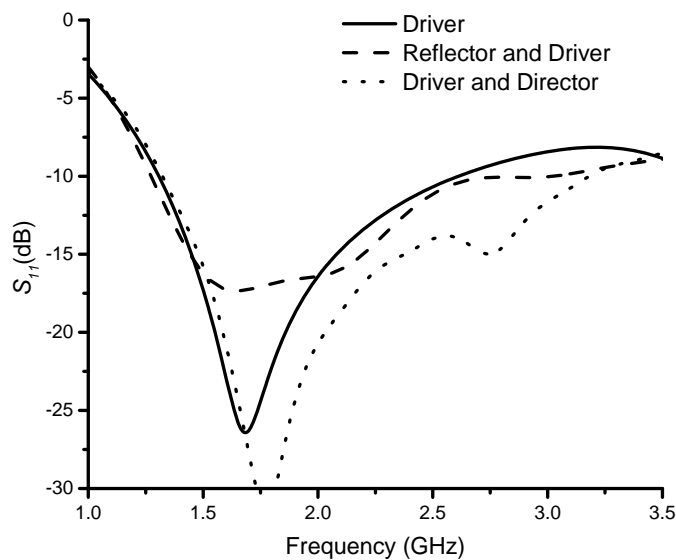
Figure 3-2. *S_{11}* vs Frequency

Simulated S_{11} for Design A, Design B, and Design C are shown in Figure 3-2 as solid, dash, and dot lines. From Figure 3-2, it is obvious that the parasitic elements are helping to enhance the bandwidth.
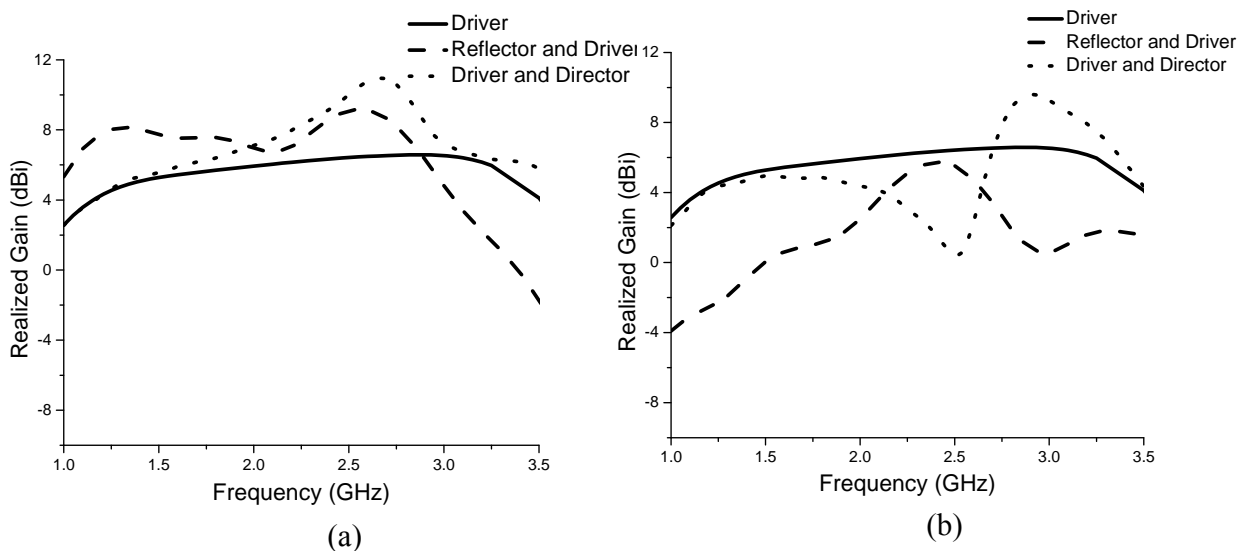
Figure 3-3. Realized gain vs frequency; (a) Forward direction, (b) Backward direction

Effect of reflector and director on directivity and realized gain can also be observed in Figure 3-3. For Design A, any direction can be considered as forward realized gain direction as it shows omnidirectional radiation pattern above the ground plane, whereas in design B the forward realized gain is in the driver direction and in design C, the forward realized gain is in the direction of the director. Figure 3-3(a) presents the forward realized gain of all three designs. From the figure, it can be observed that Design A has almost steady realized gain of around 6.0 dBi, while the Design B and Design C have their maximum realized gain to the desired directions. For Design B, average realized gain in forward direction is about 7.12 dBi over impedance bandwidth, and the maximum is about 9.15 dBi. While for design C average forward realized gain is about 7.66 dBi, and the maximum forward realized gain is about 10.97 dBi. As the director and reflector improves the directivity toward their respective desired direction, they also show effect on front to back ratio

(FBR) improvement (FBR is the difference between forward and backward realized gain, where backward refers to 180º opposite to forward). Figure 3-3(b) shows the backward realized gain of all three designs.

While design A does not have any front to back ratio, both design B and design C shows improved FBR across their operating bands as they are directive.

Analysis of Design A, Design B, and Design C have shown that bandwidth enhancement and higher directivity can be achieved by simply adding another parasitic element with the driven element. However, with only the driver and one parasitic element, high directivity and consistent realized gain cannot be achieved over the desired wider bandwidth. Therefore, the need to combine Design B and Design C is realized.
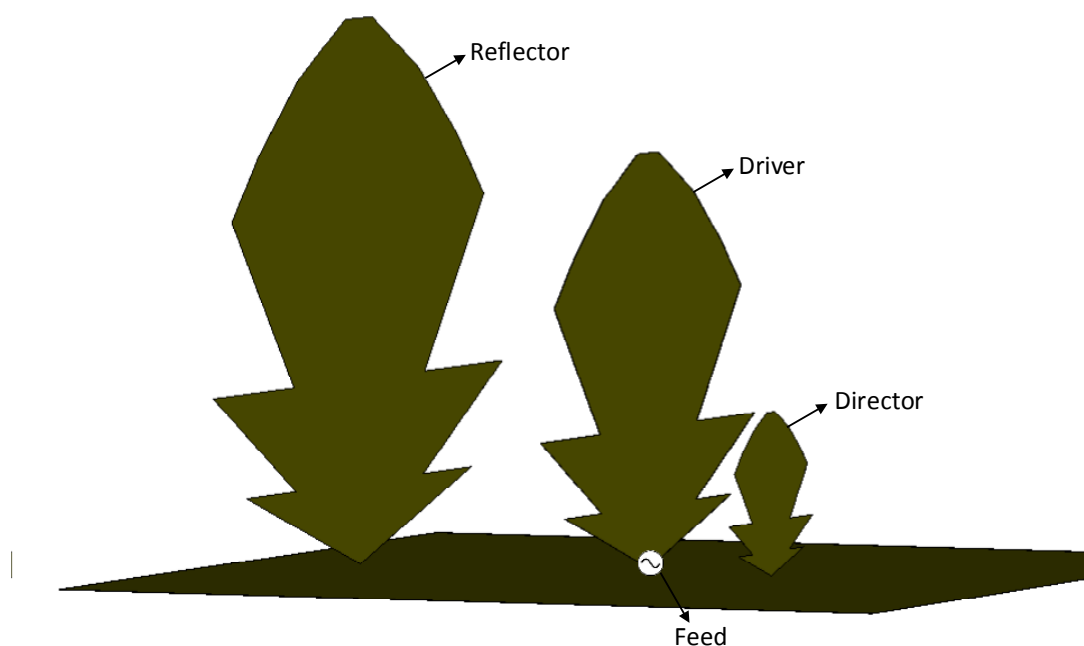

Figure 3-4. Bow-Tie Yagi antenna

The final three-element Yagi antenna design (noted as Final Design) is a combination of design B and design C. The driver and parasitic elements (reflector and director) are arranged in a Yagi structure as shown in Figure 3-4. The dimensions of the combined antenna are optimized by GA

to maximize the realized gain toward the director's direction. Antenna bandwidth with this combined configuration is expected to be much broader which can cover both Design B and Design C frequency bands. Furthermore, based on the previous analysis, it is also expected to provide consistent realized gain over the combined operating band. Except for more variables, the optimization process of the combined Yagi design is similar to that of Design B and Design C.

3.4   Simulated and Measured Result

A prototype of the antenna is fabricated on a 30 cm X 30 cm (1.28λ X 1.28λ) ground plane as shown in Figure 3-5. Bow-tie antenna elements are fabricated on a single sided DuPont Pyralux LF 9210R FPCB. The final Yagi antenna bandwidth is the combination of Design B and Design C. Simulated and measured S_{11} is shown in Figure 3-6. In simulation, the bandwidth is 86% (1.28 GHz - 3.21 GHz), while that in measurement is 84%, (1.30 GHz - 3.05 GHz). Good agreement between the simulated and measured result is observed except the 2% difference in bandwidth, which is due to fabrication error.
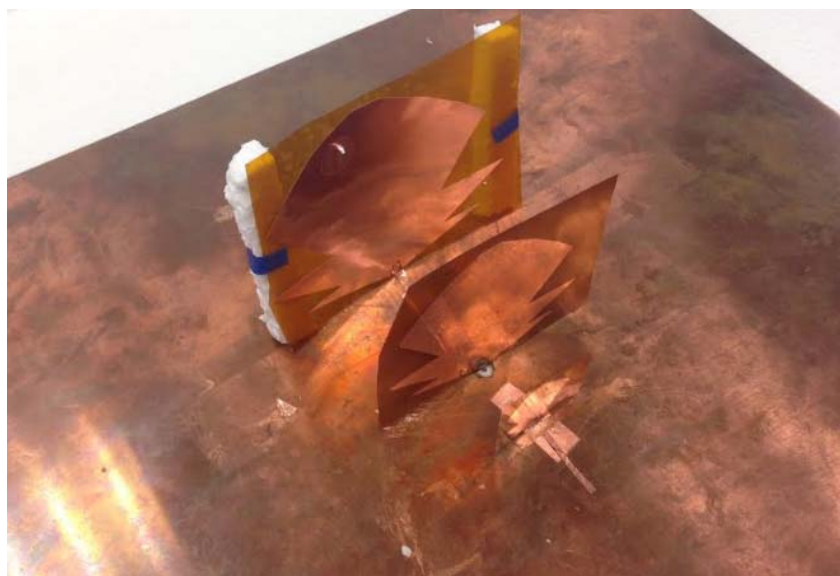
Figure 3-5. Prototype of the Bow-Tie Yagi antenna
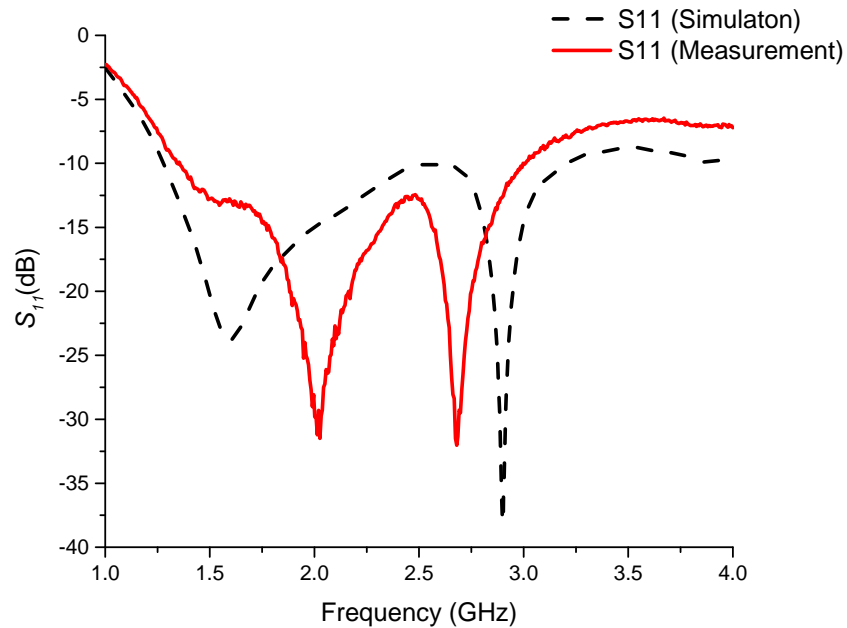
Figure. 3-6. S_{11} vs frequency

Next, the realized gain of the proposed antenna is investigated. Then, radiation patterns of the proposed antenna at selected frequencies (1.4 GHz, 1.8 GHz, 2.2 GHz, 2.6 GHz and 3.0 GHz) are measured. As the antenna is fabricated on a finite ground plane, the next step is to eliminate the finite ground plane effect from the measured results. First, five quarter wavelength monopole antennas resonating at those selected frequencies (1.4 GHz, 1.8 GHz, 2.2 GHz, 2.6 GHz and 3.0 GHz) are fabricated on a finite ground plane that has the same size as the one used for the proposed antenna (1.28λ X 1.28λ). Then, radiation pattern at those frequencies are measured, which will be used as references. Finally, the realized gain of the proposed antenna can be achieved by subtracting monopole radiation pattern from the measured radiation pattern of the proposed antenna for each corresponding frequency and then add 4.98 dBi which is maximum simulated realized gain of monopole antenna on an infinite ground plane. By this process, the finite ground plane effect can be minimized (Yu, 2013). All the realized gain measurements with simulated

realized gain patterns are shown in Figure 3-7. From the figure, it can be seen that there is a very

good agreement between the simulation and measurement.
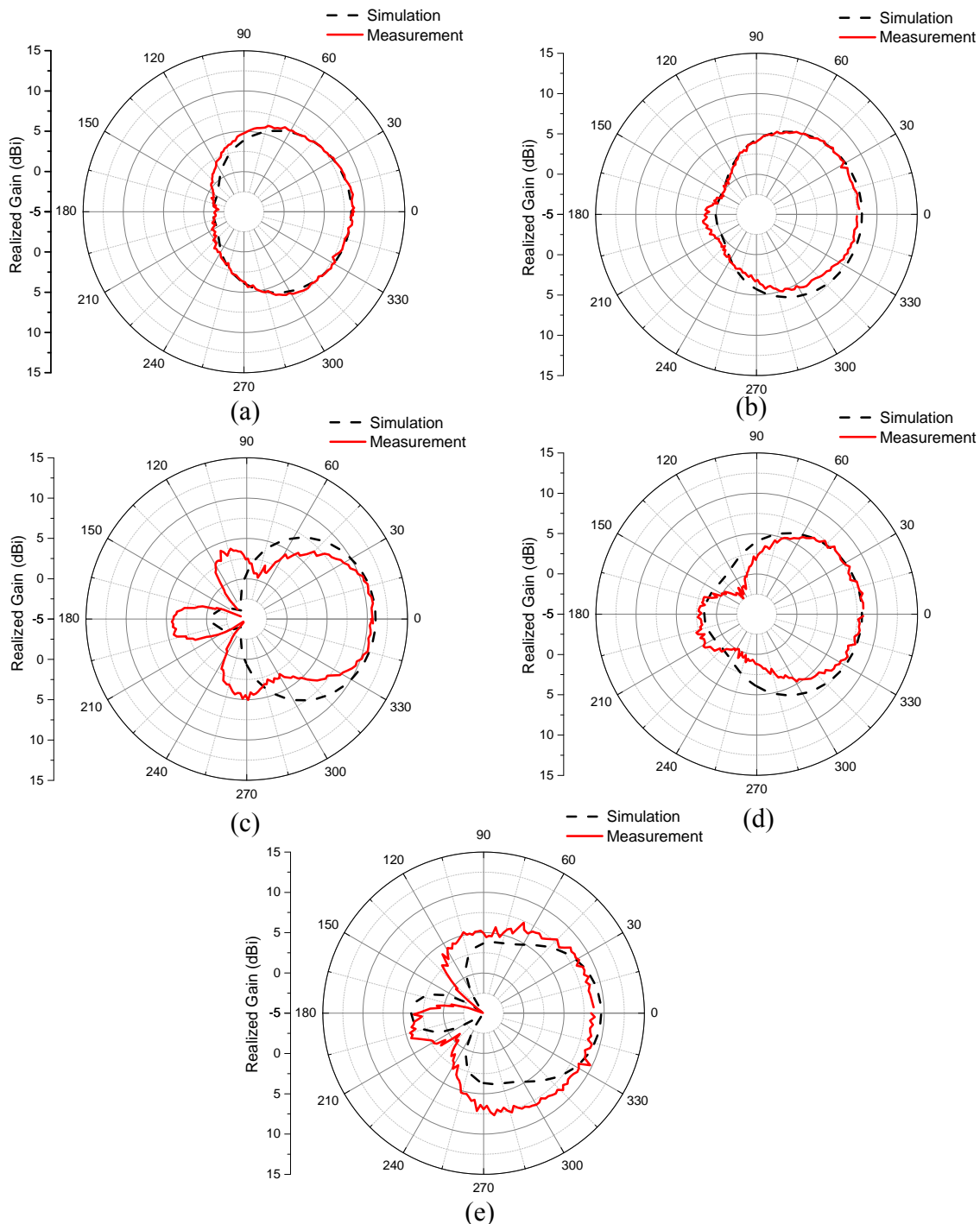
Figure 3-7. Realized gain pattern. (a) 1.4 GHz, (b) 1.8 GHz, (c) 2.2 GHz, (d) 2.6
GHz, (e) 3.0 GHz

3.5   Summary

In this section, a wideband, bow-tie Yagi antenna is proposed. The proposed Yagi antenna consists of three-elements, one is the driver and other two are the parasitic elements. A three-element wideband bow-tie antenna is used as the driver and parasite elements are the scaled version of the driver. Experiment shows that though directive pattern can be achieved with two elements Yagi design, realized gain of that antenna design is not consistent across the operating bandwidth of the antenna. To achieve a steady realized gain across the operating bandwidth, it is important to design a three-element Yagi structure. The three-element Yagi design improves the stability of the realized gain in addition to enhancing the bandwidth. For this proposed three-element Yagi antenna, measurement results agree well with the simulation results. The final antenna has a simulated fractional bandwidth of 86% (1.28 GHz -3.21 GHz), and measured fractional bandwidth of 84% (1.30 GHz- 3.05 GHz). In simulation, the average realized gain is 9.21 dBi, and maximum realized gain is 13.29 dBi.

CHAPTER 4

WIDEBAND CIRCULARLY POLARIZED LOG PERIODIC DIPOLE ARRAY ANTENNA WITH THE COMBINATION OF T-SHAPED, TOP LOADED LPDA AND BOW-TIE ANTENNA

4.1   Abstract

In this chapter, a Circularly Polarized Log Periodic Dipole Array (CPLPDA) antenna is proposed where T-shaped, top loaded LPDA antenna is orthogonally placed with a wideband bow-tie antenna to achieve bandwidth enhancement with circular polarization. The simulated impedance bandwidth is 30.1% (2.03 GHz ~ 2.75 GHz), and the axial-ratio (AR) bandwidth is 35.6% (1.93 GHz ~ 2.75 GHz). The overlapped axial-ratio and impedance bandwidth is 30.1% (2.03 GHz ~ 2.65 GHz). The average realized gain is 2.83 dBic, and the maximum realized gain is 3.17 dBic over the bandwidth in common.

4.2   Introduction

Log-periodic Dipole array (LPDA) is a popular choice for communications as it has wide bandwidth, and high gain characteristic (Isbell, 1960). By implementing a cross element design circularly polarization can be achieved where antennas communicate in both the horizontal and vertical planes in the direction of transmission (He, 2014). This concept is also applied for wideband LPDA antennas, where one set of LPDA elements is placed orthogonally with another set of LPDA elements and it is called CPLPDA. The conventional CPLPDA is designed using LPDA, which has a dipole element length of λ/2, which makes the antenna size big when a wide bandwidth is desired. To make the CPLPDA more applicable in modern wireless communication system, size reduction of the antenna is necessary. Another major problem with a CPLPDA antenna is that a two feed or a 90º phase shifted feed system is needed. To achieve circular

polarization, the current must be balanced between the vertical and horizontal components, which in most cases requires an extra component which adds to cost. Traditionally LPDA antennas are also designed having 175-200 Ω impedance matching, while designing the antenna with a standard 50 Ω matching eliminate the need for any matching transformers. Improving these features in CPLPDA would make this antenna favorable in modern communication systems.

Previously, some work has been done on LPDA antenna size reduction. A T-shaped, top loading was used to reduce the lengths of the individual dipole elements by 45% while sacrificing a gain loss of 1.5 dB compared to the conventional $\lambda/2$ element (Chen, 2017). This design was simulated and shown to work with a 10 element CPLPDA and achieving a 75% volume reduction (Haney, 2016).

Because a 90º phase shift is needed to achieve circular polarization, different methods have been implemented to achieve this characteristic. A cross dipole is shown achieving circular polarization by changing the dimensions of the radiating elements as this provides almost 90º phase shifting of the current between vertical and horizontal elements, which helps achieving circular polarization (Bolster, 1961). Wilkinson power dividers are used to create the 90º phase shift which is common among planar antennas (Lin, 2015). Circular polarization is achieved in cross-LPDA with a single feed by introducing quarter wavelength spacing between the elements and controlling the boom spacing (Wakabayashi, 1999). Though this method makes the feed design easier, it increases the overall antenna size which is not desirable.

Besides LPDA, a bow-tie antenna is a very wideband antenna. A three-element wideband antenna is introduced which has three different flare angles, thus resonates in three adjoining frequency bands and provides very wide combined bandwidth (Yen, 2016).

In this paper, a compact CPLPDA is presented where a T-shaped, top loaded size reduced LPDA is placed orthogonally with a three-element wideband bow-tie antenna. The antenna was measured in anechoic chamber using Agilent Technologies E5063A network analyzer.

4.3   Antenna Design Procedure and Simulation

For designing the conventional full-sized, $\lambda/2$ LPDA, the first element length is chosen using the lowest frequency of the desired bandwidth. Other elements length is calculated using the traditional equations (4.1) and (4.2),

$$L_n = \tau^n L_1 \tag{4.1}$$

$$d_n = 2\sigma L_n \tag{4.2}$$

$$n = 1, 2, 3\ldots\ldots n$$

Where L_1 is the first element length, L_n is the element length, d_n is the spacing between elements, n is the number of elements, σ is the spacing factor and τ is the scaling factor (Wheeler, 1947).

As the full-sized LPDA uses the half wavelength sized dipole elements, the size of this antenna is bigger. One of the most popular methods of reducing the LPDA size is T-shaped top loading and using this method the LPDA antenna volume can be reduced up to 45% (Chen, 2017).

In this proposed design, at first a six element LPDA is designed using T-shaped, top loading as shown in Figure 4-1. Then a round shaped three-element wideband bow-tie antenna is designed as shown in Figure 4-2. In the three-element bow-tie antenna design, the longest element with smallest flare angle covers the lower band of the combined bandwidth, while the middle and shortest elements cover the middle and highest bands, respectively.
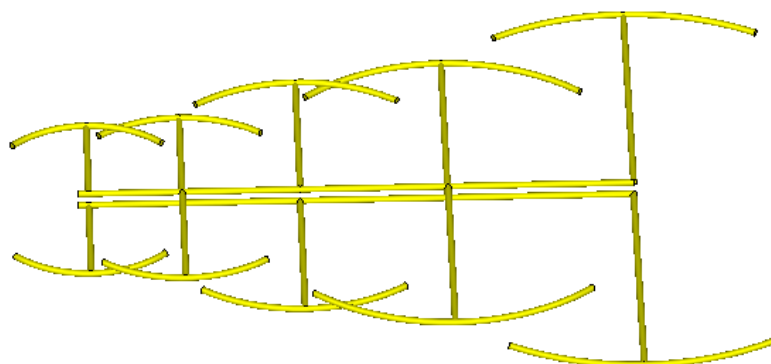
Figure 4-1. Geometry of the T-shaped, top loaded LPDA (Chen, 2014)
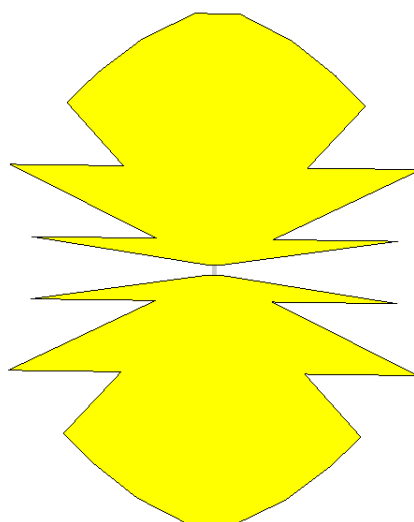
Figure 4-2. Geometry of the round shaped bow-tie antenna (Yen, 2016)

To achieve circular polarization, the T-shaped, compact LPDA and three-element bow-tie antennas are combined by placing orthogonal to each other which gives a current phase difference of around 90º. To achieve circular polarization with a standard 50Ω matching, the antenna is optimized using the genetic algorithm (GA) by varying the lengths of the dipole elements, arc length of the top loading, boom spacing and bow-tie antenna position over the boom length.

The cost functions for the optimization is defined by,

$$cost = \sum_{i=1}^{50}(S_i + 10) + 10 * (AR_i - 3) \ [dB] \tag{4.3}$$

Where S_i is the S_{11} and AR_i is the axial ratio across 50 points of the combined bandwidth of the compact LPDA and bow-tie antenna.

The geometry of the antenna is shown in Figure 4-3.
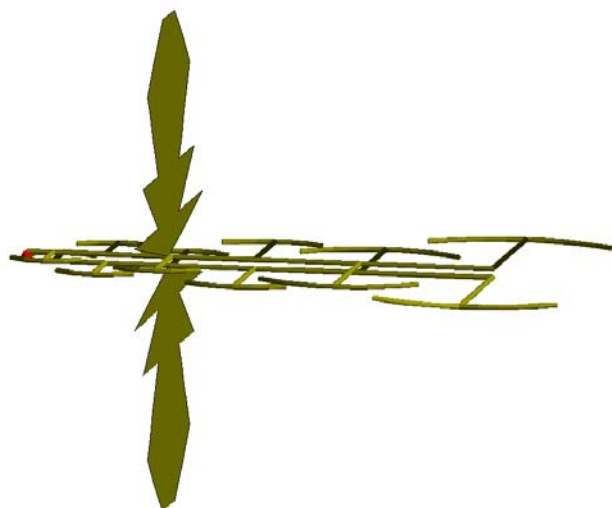
Figure 4-3. Geometry of the Combined CPLPDA with round shaped bow-tie
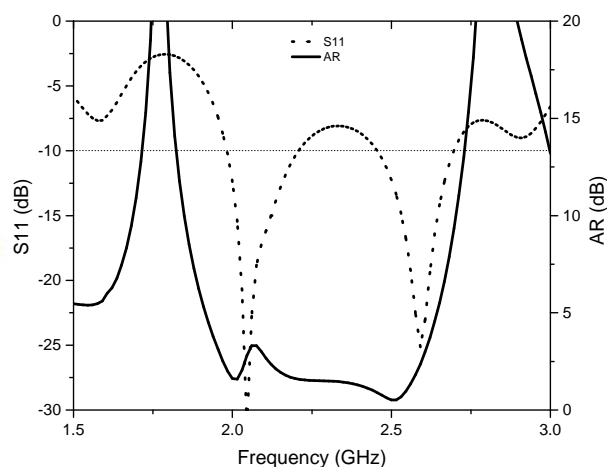
Figure 4-4. S_{11} and AR vs frequency of the Combined CPLPDA with round shaped bow-tie

The achieved S_{11} and AR of this design are shown in Figure 4-4, where S_{11} is plotted in left side of the Y axis and AR is plotted in right side of the Y axis. The achieved AR ratio bandwidth of this design is 1.93 GHz-2.74 GHz (34.7%). Achieved S_{11} bandwidth is 1.98 GHz-2.69 GHz (30.4%) except for a small bump going over -10 dB in the middle of the bandwidth. Ignoring the small bump in the middle of the S_{11} bandwidth, AR bandwidth overlaps well over the S_{11} bandwidth.

Figure 4-5. Modified (Final design) geometry of the CPLPDA

Now as this is an optimized designed, no further optimization is needed. To bring the bump under -10 dB, parametric study is done on the optimized structure. In the process of parametric study, it is observed that 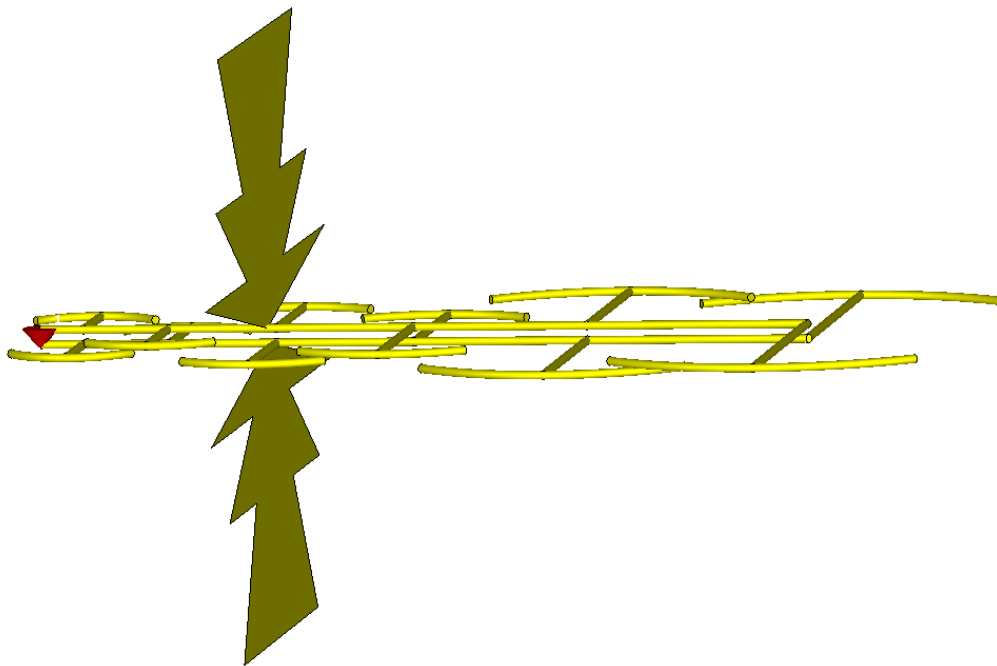truncating the top part of the round shaped bow-tie is helping in bringing the reactance part of the antenna impedance near the bump area closer to zero ohm (Ω), which in turn helps in achieving a better impedance match. It is also obvious that truncated bow-tie is helping in increasing the AR bandwidth as well. The modified CPLPDA (Final design) antenna geometry in combination of compact LPDA and truncated bow-tie is shown in Figure 4-5.

The achieved S_{11} bandwidth and AR ratio bandwidth of the modified CPLPDA antenna is shown in Figure 4-6. The achieved S_{11} bandwidth is 2.03 GHz-2.74 GHz (30.1%) and achieved AR bandwidth is 1.93 GHz- 2.74 GHz (35.2%). The overlapped bandwidth of the S_{11} and AR bandwidth is 2.03 GHz-2.74 GHz (30.1%).
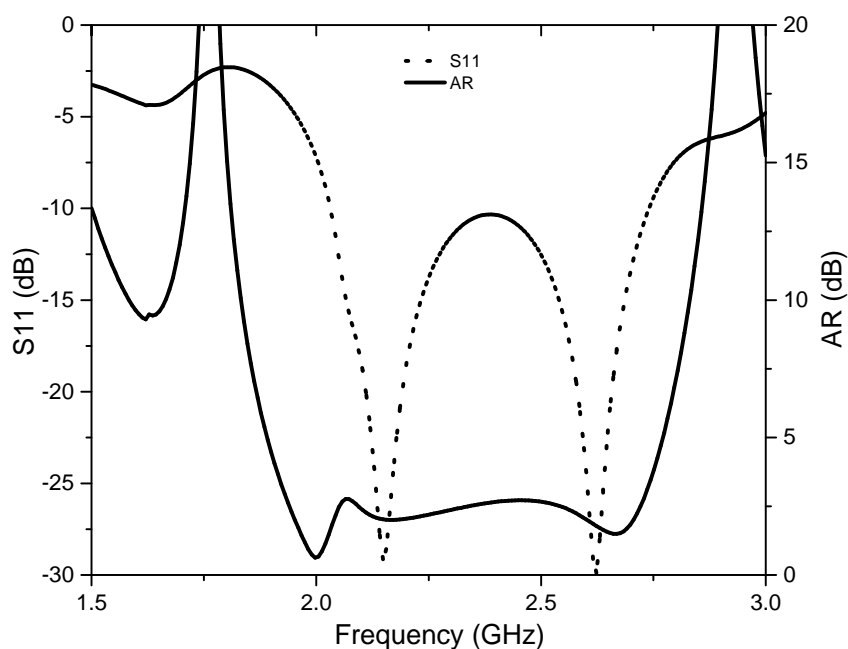
Figure 4-6. S_{11} and AR vs frequency (Final design)

4.4 Measurement Verification

A prototype of the compact CPLPDA is fabricated for verification with measurement. Figure 4-7, depicts fabricated prototype of the antenna. The bow-tie antenna is fabricated on single-sided DuPont Pyralux LF 9210R FPCB using the etching process. The T-shaped, top loaded LPDA antenna is fabricated using 18 AWG (0.5 mm) copper wire. The antenna is constructed using balsa wood support ($\varepsilon r = 1.22$) which has negligible effect on the antenna performance.

For the measurement purpose, to calibrate the network analyzer, a 180º hybrid coupler (Krytar, model 4005070, frequency band: 0.5 GHz ~ 7 GHz) is used. Two coaxial cables are connected to the -3-dB input ports of the hybrid coupler through SMA connectors and then the measurement is calibrated at the end of these coaxial cables to extinguish any effect of the coaxial cable and coupler on the measurement result.
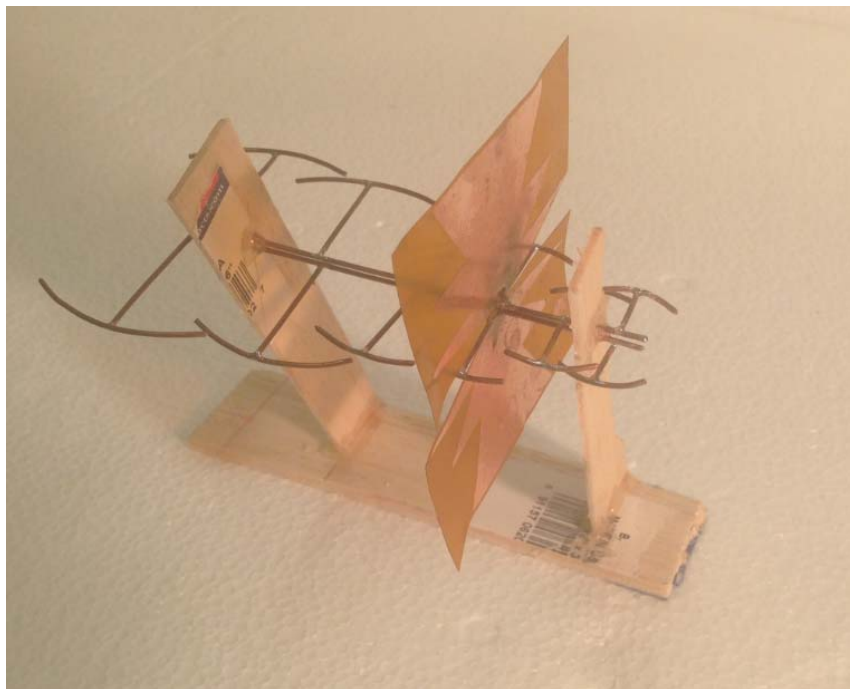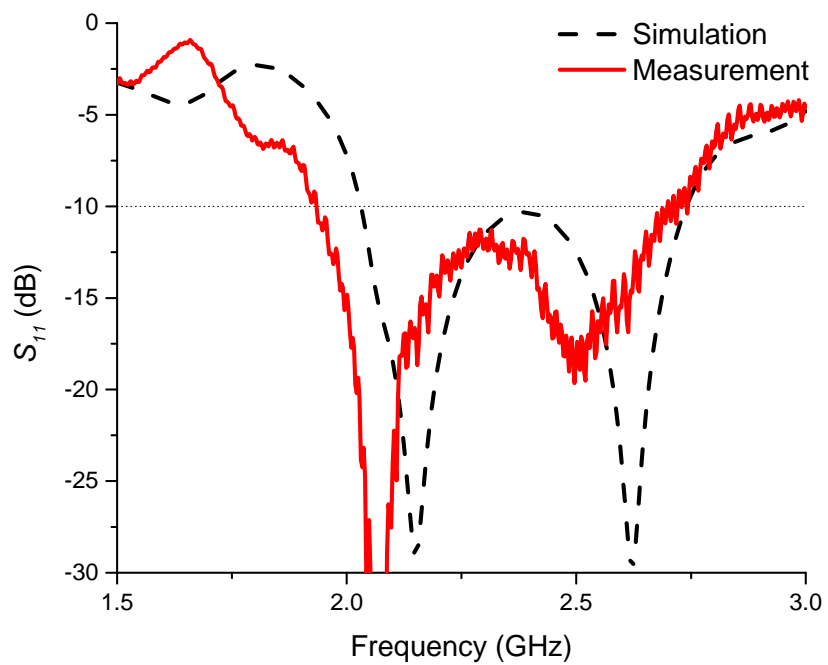
Figure 4-7. Prototype of the CPLPDA

Figure 4-8. Simulated and measured S_{11} of the Final CPLPDA design

The measured S_{11} for the final CPLPDA design is shown in Figure 4-8 with the simulated S_{11} for direct comparison. The measured S_{11} of the compact CPLPDA is 34.0% (1.93 GHZ- 2.72GHz) and simulated S_{11} is 30.1% (2.03 GHz- 2.75 GHz). A good agreement is observed between simulation and measured results except a little shift of the S_{11} graph to the left. Soldering loss and small fabrication error could be the reason for the shifting.

Then the farfield radiation pattern of the antenna is measured. The measured and simulated AR of the antenna is shown in Figure 4-9. Measured AR ratio bandwidth is 33.5% (1.91 GHz- 2.68 GHz) and simulated AR bandwidth is 35.6% (1.93 GHz- 2.75 GHz). It is obvious that the simulated and measured results match very well.

Measured and simulated realized gain pattern is presented in Figure 4-10, Figure 4-11 and Figure 4-12 at 2.1 GHz, 2.4 GHz, and 2.7 GHz, respectively, where average realized gain over the common impedance and axial ratio bandwidth is 2.83 dBic. Measured and simulated realized gain patterns agree very well in all three frequencies at both the xz and yz planes. Measurement has been taken in an anechoic chamber using a high-frequency ENA series vector network analyzer.
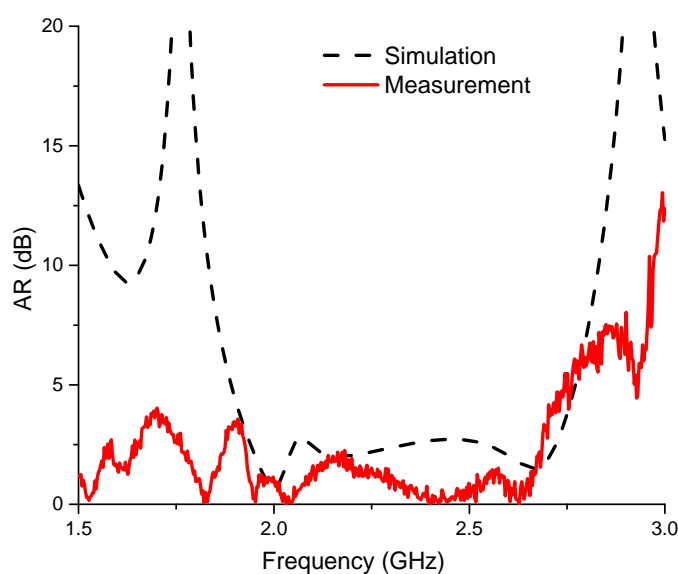
Figure 4-9. Simulated and measured AR of the Final CPLPDA design

E_θ

E_Φ

$\sqrt{(E_\theta)^2 + (E_\Phi)^2}$

(a)

E_θ

E_Φ

$\sqrt{(E_\theta)^2 + (E_\Phi)^2}$

(b)
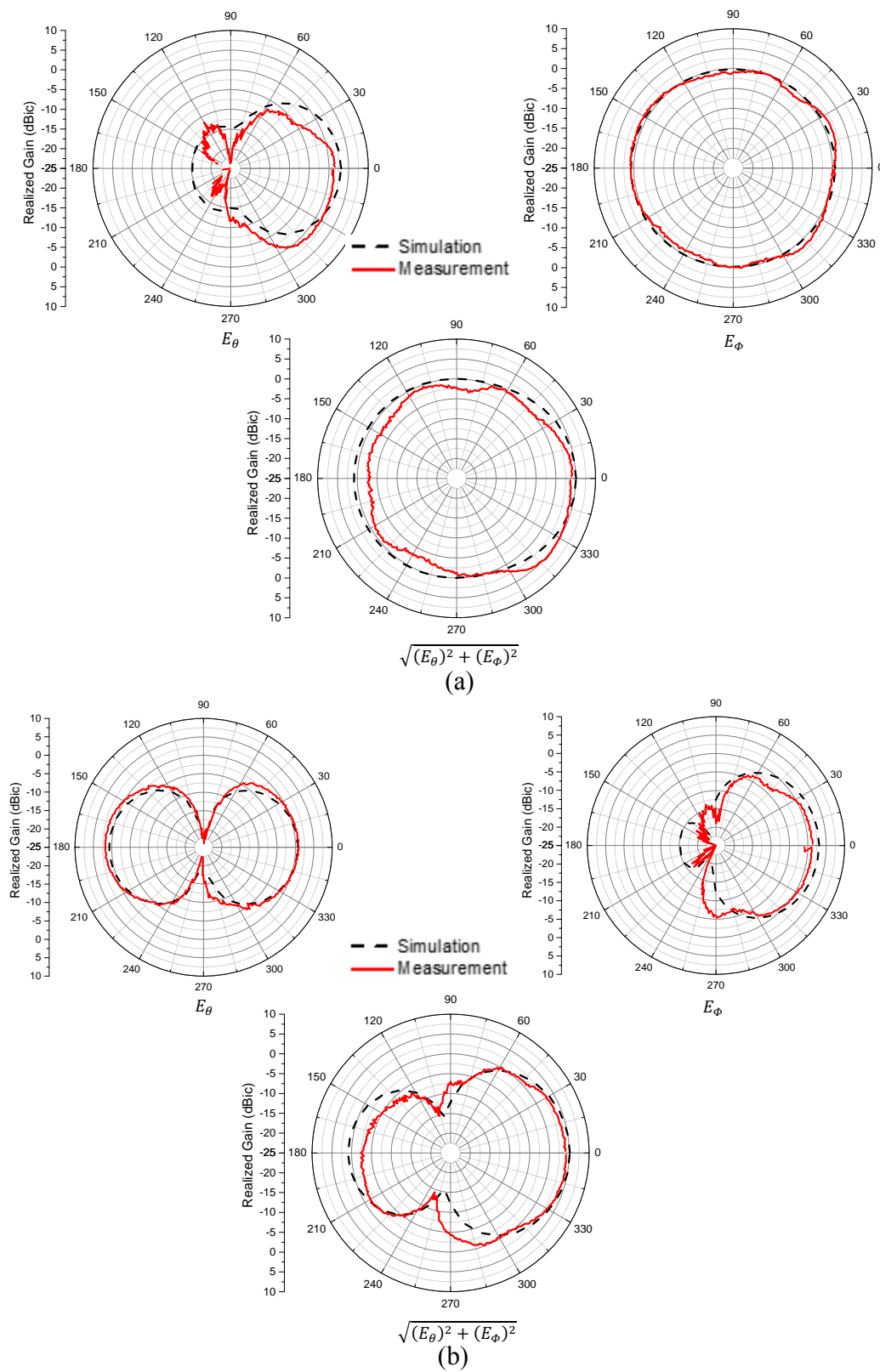
Figure 4-10. Realized gain pattern at 2.1 GHz. (a) xz plane, (b) yz plane.

$$\sqrt{(E_\theta)^2 + (E_\Phi)^2}$$

(a)

$$\sqrt{(E_\theta)^2 + (E_\Phi)^2}$$

(b)
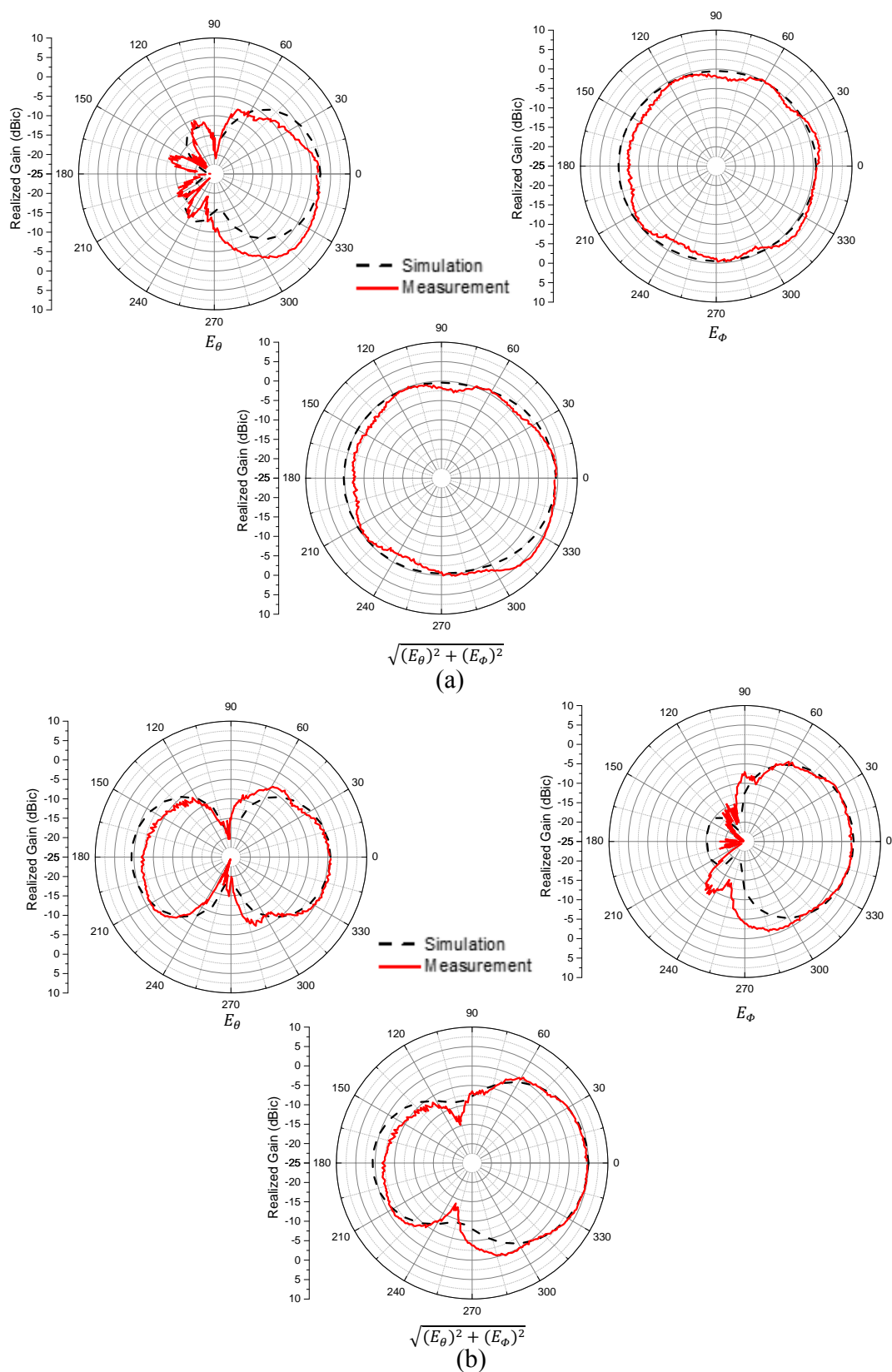
Figure 4-11. Realized gain pattern at 2.4 GHz. (a) xz plane, (b) yz plane.

E_θ

E_Φ

$\sqrt{(E_\theta)^2 + (E_\Phi)^2}$

(a)

E_θ

E_Φ

$\sqrt{(E_\theta)^2 + (E_\Phi)^2}$

(b)
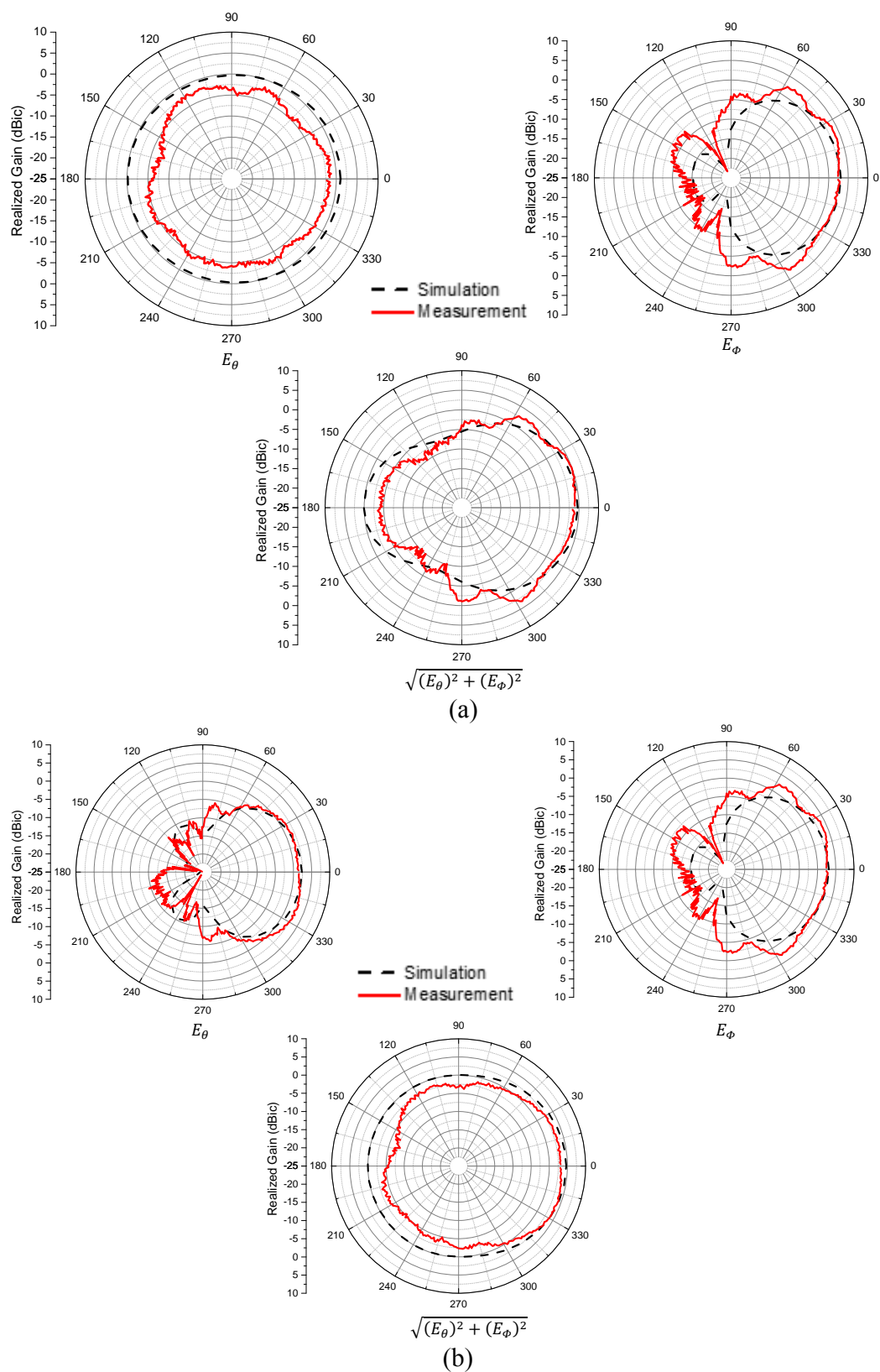
Figure 4-12. Realized gain pattern at 2.7 GHz. (a) xz-plane, (b) yz-plane.

4.5   Summary

Design of a two-planar structured CPLPDA antenna is discussed in this chapter. A three-element wideband bow-tie antenna and a LPDA antenna with T-shaped, top loaded elements are placed orthogonally to each other to achieve circular polarization. A prototype was fabricated and measured. There is good agreement between the simulated and measured results. This compact CPLPDA antenna achieved fractional impedance bandwidth of 30.1% and axial ratio bandwidth of 35.6% in simulation. The average realized gain is 2.83 dBic and the peak realized gain is 3.17 dBic over the common impedance and axial ratio bandwidth.

CHAPTER 5

CONCLUSION

5.1   Summary

In this thesis, antenna design methods were shown on how to implement those to achieve high directivity, impedance matching for wider bandwidth, pattern reconfigurability, and circular polarization. Chapter 1 provides background discussion of bow-tie antenna design, and its bandwidth enhancement techniques. Finally, the measurement set up and equipment used for the antenna fabrication and measurement is discussed.

In chapter 2, a wideband pattern reconfigurable antenna using the bow-tie antenna was shown. At first, a three-element wideband bow-tie antenna was designed to implement as the driver and other two triangular shaped bow-tie antennas were used as the reflector elements. A prototype of the antenna was fabricated, and antenna parameters were measured. Good agreement was found between the simulated and measured results. This antenna achieved simulated bandwidth of 45.01% (1.45 GHz-2.27 GHz) and measured bandwidth of 46.5 %(1.39 GHz-2.27 GHz).

In chapter 3, a Yagi antenna design with wideband characteristics is presented. The antenna consists of three elements, the driver, and parasitic elements (reflector, and director). A three-element wideband bow-tie antenna is implemented for the driver, and reflector and the driver are the scaled version of the driver. The simulated and measured bandwidth of the antenna are 86% and 84% respectively. Measured radiation patterns were also in a good agreement with the simulated radiation pattern.

Chapter 4 presented a method of designing a CPLPDA antenna with the combination of T-shaped, top loaded LPDA and a three-element wideband bow-tie antenna. In this design, a single feed was used to achieve circular polarization. A prototype was fabricated and measured. There is good agreement between the simulated and measured results. This compact CPLPDA achieved impedance bandwidth is 30.1% and axial ratio bandwidth is 35.2%.

5.2   Future Work

Future work in these studies, would be decreasing the size of the antenna by reducing the spacing between the elements. The improvement of the gain of the Yagi antenna can be done by doing more parametric study on the director.

Future work in case of the CPLPDA antenna would be to improve the impedance bandwidth and the axial ratio bandwidth of a CPLPDA antenna by doing more parametric study on the bow-tie and the top-loading of the LPDA.

REFERENCES

Anagnostou, D.E. Papapolymerou, J. Tentzeris, M.M. Christodoulou, C.G., "Wideband Antenna Design and Fabrication for Modern Wireless Communications Systems," in *Elsevier, IEEE*, vol.11, no., pp.348-353, 2013.

W. L. Stutzman and G. A. Thiele, Antenna Theory and Design, 3rd ed. New York: John Wiley & Sons, Inc., 2013.

H.G. Schantz, "A Brief History of UWB Antennas," IEEE AES Systems Mag., vol. 19, no. 4, pp. 22-26, 2004.

Chu, L. J. "Physical limitations of omni-directional antennas". Journal Applied Physics 19: 1163–1175 December 1948.

A. A. Eldek, A. Z. Elsherbeni, and C. E. Smith, "Wideband bow-tie slot antenna with tuning stubs", Proc. IEEE Radar Conf., pp. 583-588, 2004.

K. M. Z. Shams, and M. Ali, "A cpw-fed inductively coupled modified bow-tie slot antenna", IEEE Antennas Propagation Society Int. Symp., vol. 3B, pp. 365-368, 2005.

William H. Hayt and J. A. Buck, Engineering Electromagnetics, 8th ed. McGraw‑Hill Education, 2011.

Constantine A. Balanis, Modern Antenna Handbook, John Wiley & Sons, 2011.

M. Jusoh, T. Aboufoul, T. Sabapathy, A. Alomainy, and M. R. Kamarudin," Pattern-Reconfigurable Microstrip Patch Antenna With Multidirectional Beam for WiMAX Application ", IEEE Antennas and Wireless Propagation Letters, vol. 13, 2014.

S. M. Lee, J Ahn, Y. J. Yoon," Pattern reconfigurable antenna for Wireless LAN dual-band," International Conference on ICT Convergence (ICTC), Jeju Island, 2012, pp. 447-448.

S.D. Assimmonis, A. Theopoulos, and T. Samaras, "A new high-gain and low-complexity pattern-reconfigurable antenna," 9th European Conf. Antennas and propag. (EuCAP), Lisbon, 2015.

D. Arceo and C. A. Balanis,"A compact Yagi–Uda antenna with enhanced bandwidth," IEEE Antennas Wireless Propag. Lett., vol. 10, pp 442–445, 2011.

KEYSIGHT technologies, Agilent 5063A Network Analyzer, Accessed March 7, 2017, http://www.keysight.com/en/pdx-x202023-pn-E5063A/ena-series-network-analyzer?cc=US

DuPont USA LLC,"DuPont™ Pyralux® LF Copper-Clad Laminates flexible composites", Accessed March 3, 2016, http://www.dupont.com/content/dam/dupont/products-andservices/ electronic-and-electrical-materials/flexible-rigid-flex-circuitmaterials/ documents/PyraluxLFclad_DataSheet.pdf, 2016.

Lim and S. Lim, "Monopole-like and boresight pattern reconfigurable antenna," IEEE Trans. Antennas Propag., vol. 61, no. 12, pp. 5854-5859, Dec. 2013.

X.-S. Yang, B.-Z. Wang, W.-X. Wu, and S.-Q. Xiao, "Yagi patch antenna with dual-band and pattern reconfigurable characteristics," IEEE Antennas and Wireless Propagation Letters, vol. 6, pp. 168-171, 2007.

L. Inseop and L. Sungjoon, "Monopole-like and boresight pattern reconfigurable antenna," IEEE Trans. Antennas Propag., vol. 61, pp. 5854-5859, 2013.

Haney, J.; Lim, S., "A miniturized, circularly polarized log periodic dipole array," 2016 International Workshop on Antenna Technology (iWAT), Cocoa Beach, FL, pp. 80-81, 2016.

X. Cai, A. G. Wang, N. Ma, and W. Leng, "A novel planar parasitic array antenna with reconfigurable azimuth pattern," IEEE Antennas Wireless Propag. Lett., vol. 11, pp. 1186–1189, Oct. 2012.

Y. Li, Z. Zhang, J. Zheng, Z. Feng, and M. F. Iskander, "Experimental analysis of a wideband pattern diversity antenna with compact reconfigurable CPW-to-slotline transition feed," IEEE Trans. Antennas Propag., vol. 59, no. 11, pp. 4222–4228, Nov. 2011.

S. J. Shi and W. P. Ding, "Radiation pattern reconfigurable microstrip antenna for WiMAX application," Electron. Lett., vol. 51, no. 9, pp. 662– 664, Apr. 2015.

Z. Li, E. Ahmed, A. M. Eltawil, and B. A. Cetiner, "A beam-steering reconfigurable antenna for WLAN applications," IEEE Trans. Antennas Propag., vol. 63, no. 1, pp. 24–32, Jan. 2015.

M. S. Alam, and A. M. Abbos, "Wideband Pattern-Reconfigurable Antenna Using Pair of Radial Radiators on Truncated Ground With Switchable Director and Reflector," IEEE Trans. Antennas Propag., vol. 63, no. 1, pp. 24–32, Jan. 2015.

S. A. Rezaeieh, M. A. Antoniades, and A. M. Abbosh, "Miniaturized Planar Yagi Antenna Utilizing Capacitively Coupled Folded Reflector, vol. 16, no. 1, pp. 1977-1980, Apr. 2017.

R. J. Fontana, "Recent system applications of short-pulse ultra-wideband (UWB) technology," IEEE Trans. Microw. Theory Tech, vol. 52, no. 9, pp. 2087–2104, Sep. 2004.

J. J. Yu and S. Lim, "Design of multi-band, compact parasitic array with twisted, helical directors," IEEE Trans. Antennas Propag., vol. 61, no. 1, pp. 444–449, Jan. 2013.

Wakabayashi, R.; Shimada, K.; Kawakami, H.; Sato, G., "Circularly polarized log-periodic dipole antenna for EMI measurements," in Electromagnetic Compatibility, IEEE Transactions on, vol.41, no.2, pp.93-99, May 1999.

He, Y.; He, W.; Wong, W., "A Wideband Circularly Polarized Cross-Dipole Antenna," IEEE Antennas Wireless Propag. Lett., vol.13, no., pp.67-70, 2014.